



HAL
open science

Design, synthesis and evaluation of enzyme-responsive fluorogenic probes based on pyridine-flanked diketopyrrolopyrrole dyes

Sébastien Jenni, Flavien Ponsot, Pierre Baroux, Lucile Collard, Takayuki Ikeno, Kenjiro Hanaoka, Valentin Quesneau, Kévin Renault, Anthony Romieu

► To cite this version:

Sébastien Jenni, Flavien Ponsot, Pierre Baroux, Lucile Collard, Takayuki Ikeno, et al.. Design, synthesis and evaluation of enzyme-responsive fluorogenic probes based on pyridine-flanked diketopyrrolopyrrole dyes. *Spectrochimica Acta Part A: Molecular and Biomolecular Spectroscopy* [1994-..], 2021, 248, pp.119179. 10.1016/j.saa.2020.119179 . hal-03935733

HAL Id: hal-03935733

<https://u-bourgogne.hal.science/hal-03935733>

Submitted on 12 Jan 2023

HAL is a multi-disciplinary open access archive for the deposit and dissemination of scientific research documents, whether they are published or not. The documents may come from teaching and research institutions in France or abroad, or from public or private research centers.

L'archive ouverte pluridisciplinaire **HAL**, est destinée au dépôt et à la diffusion de documents scientifiques de niveau recherche, publiés ou non, émanant des établissements d'enseignement et de recherche français ou étrangers, des laboratoires publics ou privés.

Design, synthesis and evaluation of enzyme-responsive fluorogenic probes based on pyridine-flanked diketopyrrolopyrrole dyes

Sébastien Jenni^{a,†,*}, Flavien Ponsot^{a,†}, Pierre Baroux^a, Lucile Collard^a, Takayuki Ikeno^b, Kenjiro Hanaoka^b, Valentin Quesneau^a, Kévin Renault^a, Anthony Romieu^{a,*}

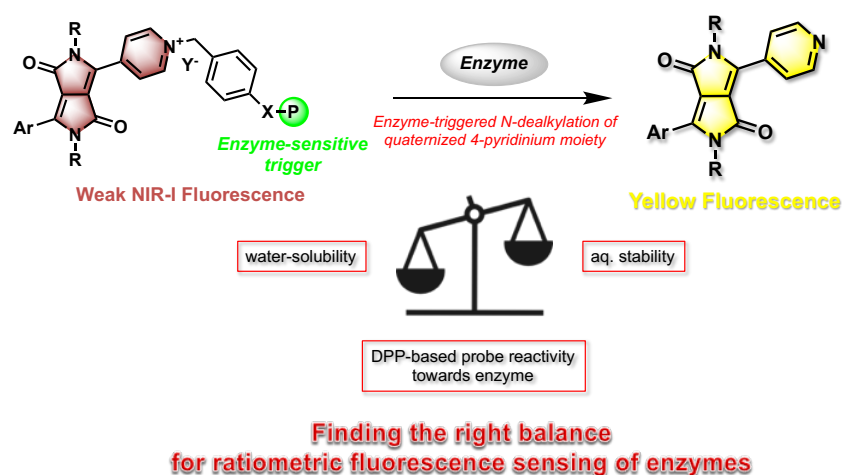
^aInstitut de Chimie Moléculaire de l'Université de Bourgogne, UMR 6302, CNRS, Univ. Bourgogne Franche-Comté, 9, Avenue Alain Savary, 21000 Dijon, France

^bGraduate School of Pharmaceutical Sciences, The University of Tokyo, Tokyo 113-0033, Japan

ABSTRACT

The ever-growing demand for fluorogenic dyes usable in the rapid construction of analyte-responsive fluorescent probes, has recently contributed to a revival of interest in the chemistry of diketopyrrolopyrrole (DPP) pigments. In this context, we have explored the potential of symmetrical and unsymmetrical DPP derivatives bearing two or one 4-pyridyl substituents acting as optically tunable group(s). The unique fluorogenic behavior of these molecules, closely linked to *N*-substitution/charge state of their pyridine unit (*i.e.*, neutral pyridine or cationic pyridinium), has been used to design DPP-based fluorescent probes for detection of hypoxia-related redox enzymes and penicillin G acylase (PGA). In this paper, we describe synthesis, spectral characterization and bioanalytical validations of these probes. Dramatic differences in terms of aqueous stability and enzymatic fluorescence activation were observed. This systematic study enables to delineate the scope of application of pyridine-flanked DPP fluorophores in the field of enzyme biosensing.

Graphical abstract



[†] These authors contributed equally to this work.

* Corresponding authors. Tel. +33 3-80-39-90-44 (S. J.) 36-24 (A. R.); e-mail sebstien.jenni@u-bourgogne.fr and anthony.romieu@u-bourgogne.fr

Keywords Diketopyrrolopyrrole; Enzyme detection; Fluorogenic probe; Hypoxia; Penicillin G acylase; Reductase

Highlights

DPP-based fluorescent probes with self-immolative 4-aminobenzyl quaternary pyridinium were synthesized

DPP-based fluorescent probes based on fully quaternized 3,6-bis-(4'-pyridyl)-DPP are not stable in aq. solution

DPP-based fluorescent probes for hypoxia detection are not reactive towards AzoR and NTR

A DPP-based ratiometric fluorescent probe for penicillin G acylase detection was developed

Activation mechanism of PGA-sensitive probe was deciphered by RP-HPLC-fluorescence/MS

1. Introduction

Over the past decade, intensive research efforts have been devoted to develop novel high-performance visible fluorescent organic dyes based on the diketopyrrolopyrrole (DPP) framework which was used previously only as basic structural element of pigment for paints, coatings and printing inks industry [1]. The high degree of interest for these photoactive bis-lactam-based small molecules is related to their numerous valuable features including facile synthetic accessibility, ease of structural modification, outstanding chemical and thermal robustness and attractive spectral properties [2]. However, compared with common classes of organic-based fluorophores (*i.e.*, BODIPY, coumarin, cyanine and xanthene dyes) [3], the main limitation currently associated with the fluorescent DPP dyes is the lack of simple and effective structural alteration strategies to readily tune their emission capability, especially after their specific interaction or reaction with a biological and/or reactive species to be detected. Modulation of fundamental photophysical processes as the final result of such activity-based sensing approaches, is the key to the design of analyte-responsive fluorescent probes applied to sensing/imaging applications [4]. Nevertheless, there are some interesting achievements focusing on fluorogenic detection of reactive analytes (*e.g.*, Hg(II) cations, H₂S and biothiols) both *in vitro* and in living cells through irreversible and stoichiometric organic reactions. However, as illustrated by the selected examples shown in Fig. 1 [5], the corresponding DPP-based fluorescent chemodosimeters are not constructed from a common and structurally simple fluorogenic scaffold bearing an optically tunable group (*e.g.*, amino, hydroxyl, ...) as is frequently the case for reaction-based fluorescent probes using coumarins, cyanines or xanthenes as photoactive reporters [6]. In an effort to address this gap, the Hua group has recently proposed an unsymmetrical 3,6-diaryl-DPP core structure bearing a single 4'-pyridyl unit acting as fluorogenic reactive center [7] (Fig. 1). Indeed, depending on the charge state of this *N*-heterocycle (*i.e.*, pyridinium cation bearing *N*-alkyl substituent and neutral pyridine molecule), internal charge transfer (ICT) process is operative or completely abolished. Thus, a ratiometric detection strategy of enzymes (esterase activity and γ -glutamyltranspeptidase (γ -GT)) [7a, 7c] and reactive oxygen species (ROS) such as superoxide radical anion (O₂^{•-}) [7b], through an effective biocompatible domino reaction triggered by the targeted bioanalyte and leading to *N*-dealkylation of 4'-pyridinium moiety, has been devised and applied to living cells and *in vivo* context. To the best of our knowledge, these contributions are the only examples of enzyme-responsive DPP probes that, in addition, highlight the potential of these less common

activatable fluorophores for biological imaging applications. However, curiously no attention has been paid to optimization of their physicochemical properties (*e.g.*, water solubility) [8] for better performances in aq. media whereas some effective strategies for imparting polarity and possibly bioconjugation ability to DPP derivatives are readily available in the literature [9]. In pursuit of novel structurally simple fluorophores possessing both biocompatibility and fluorogenic reactivity, the chemistry of pyridine-flanked DPP dyes deserves to be revisited. Furthermore, this will enable to assess the level of versatility of this emerging class of fluorescent platforms, particularly illustrated by the range of different enzymes (both peptidases and reductases) which could be detected.

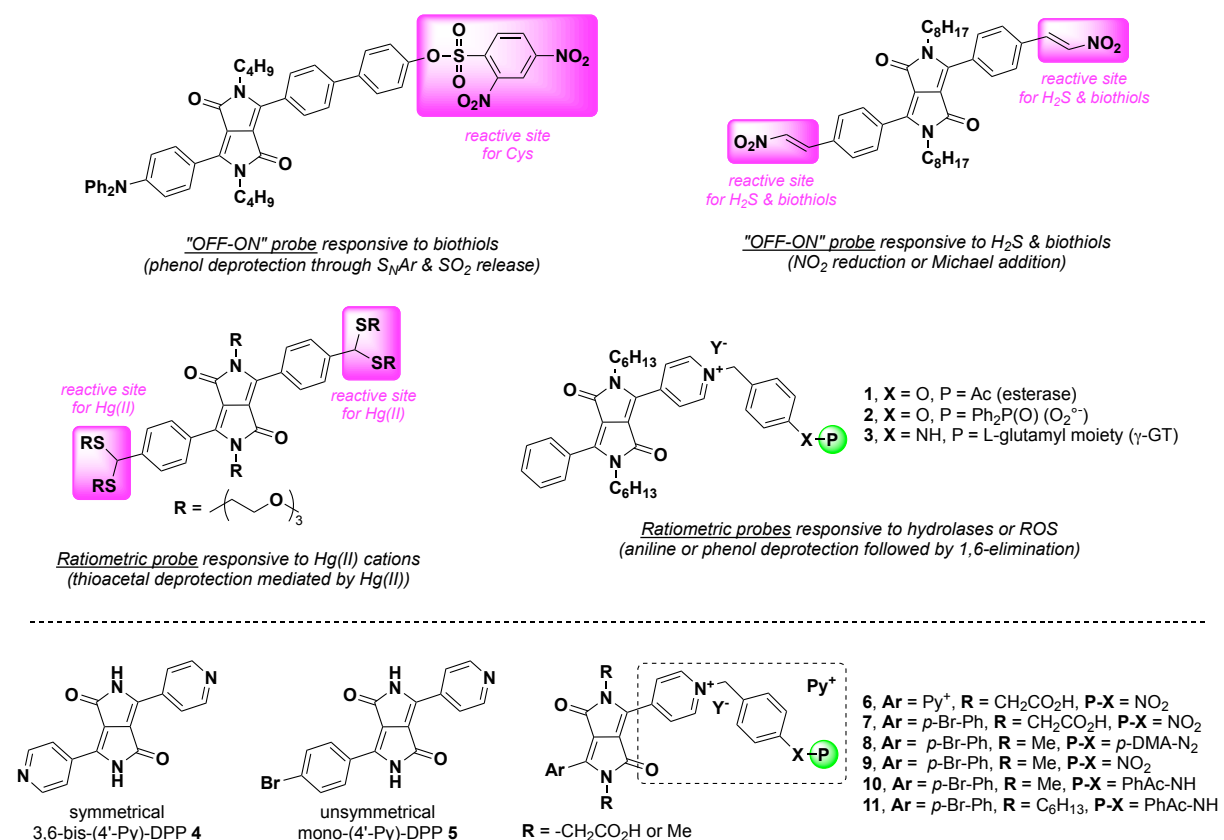


Fig. 1. Selected examples of DPP-based fluorescent chemodosimeters (top) [5, 7]; structures of pyridine-flanked DPP pigments and related enzyme-responsive fluorogenic probes studied in the present work (bottom) (Cys = L-cysteine, Ac = acetyl, γ -GT = γ -glutamyltranspeptidase, Py = pyridyl, *p*-Br-Ph = *p*- or 4-bromophenyl, *p*-DMA- N_2 = 2-[4-(dimethylamino)phenyl]diazeny], PhAc = phenylacetyl, for compounds 1-3, the nature of counter-ion Y^- was not specified by the authors, for 6-11, $Y^- = CF_3CO_2^-$).

The present Article comes within this topic. Indeed, we report the synthesis of six different enzyme-responsive fluorogenic DPP probes rationally designed from symmetrical 3,6-bis-(4'-pyridyl)-DPP pigment 4 or an unsymmetrical analog namely mono-(4'-pyridyl)-DPP pigment 5. They differ in both the type of their bio-metabolizable recognition moiety with the aim of targeting hypoxia-related reductases (azo- and nitroreductase, AzoR and NTR respectively) or

penicillin G acylase (PGA) [10], and the nature of their *N*-lactam substituents (*i.e.*, carboxymethyl, methyl and hexyl) directly impacting the solubility and the photophysical behavior of the probes in aq. environments (Fig. 1). However, the common feature of all probes related to their activation mechanism, is the transient formation of a highly reactive 4-aminobenzyl quaternary pyridinium intermediate readily prone to self-immolation [11]. The fluorogenic behavior as well as enzymatic activation and aq. stability of these DPP probes were studied through *in vitro* fluorescence assays and HPLC-fluorescence/-MS analyses. In the light of results and data produced, we will identify suitable combination of structural elements to achieve conversion of early industrial DPP pigments to high-performance fluorescent probes for tracking enzymatic activities in living systems [10, 12].

2. Experimental Section

See SI for all experimental details related to the preparation of compounds **4**, **5**, **11**, **19-21**, photophysical characterizations and HPLC analyses/purifications.

2.1. General

Unless otherwise noted below, all commercially available reagents and solvents were used without further purification. TLC were carried out on Merck DC Kieselgel 60 F-254 aluminum sheets. The spots were directly visualized and through illumination with dual wavelength UV lamp ($\lambda = 254$ and 365 nm). Column chromatography purifications were performed with different types of silica gel for which specifications are given throughout the description of synthetic protocols. MeCN and THF were dried over alumina cartridges immediately prior to use, using a solvent purification system PureSolv PS-MD-5 model from Innovative Technology. DMF (Fisher Chemicals, extra pure, $\geq 99\%$, #D/3840/17) was dried by storage over activated 3 Å molecular sieves and kept under Ar atmosphere. Anhydrous NMP over 3 Å molecular sieves was purchased from Acros Organics. DMSO (for spectrophotometry, #D5293) was purchased from TCI Europe. Formic acid (puriss p.a., ACS reagent, reagent Ph. Eur., $\geq 98\%$, #33015), NTR (from *Escherichia coli*, #N9284, 0.1 U/ μ g, lyophilized enzyme + buffer resuspended in ultrapure water), NADH and LAP (microsomal, from porcine kidney, #L5006, type IV-S, ammonium sulfate suspension, 10-40 U per mg protein) were obtained from Merck-Millipore (brand Sigma-Aldrich) and stored at -20 °C for NTR/NADH and LAP. PGA (from *Escherichia coli*, EZ50150, 841 U/mL) was provided by Iris Biotech GmbH. The HPLC-

gradient grade MeCN was obtained from Carlo Erba, Fisher Scientific or VWR. Aq. buffers and aq. mobile-phases for HPLC were prepared using ultrapure water produced by an ELGA PURELAB Ultra system (purified to 18.2 M Ω .cm).

2.2. Instruments and methods

Centrifugation operations were performed with a Thermo Scientific Espresso Personal Microcentrifuge instrument. Centrifugation steps required for isolation of DPP pigments **4** and **5** were performed with an Hettich Universal 320 instrument (with the following parameters: 15 min, 3000 rpm). ^1H -, ^{13}C - and ^{19}F -NMR spectra were recorded on Bruker spectrometers: Avance Neo 500 MHz equipped with a 5 mm BBOF iProbe and Avance III HD 600 MHz equipped with a 5 mm BBOF N₂ cryoprobe. NMR spectroscopy chemical shifts are quoted in parts per million (ppm) relative to TMS (for ^1H , and ^{13}C) and CFCl_3 (for ^{19}F). For ^1H and ^{13}C spectra, calibration was made by using residual signals of partially deuterated solvent summarized by Fulmer *et al.* [13]. J values are expressed in Hz. ^{13}C substitutions of some compounds (**16** and **18**) were determined with JMOD experiments, differentiating signals of methyl and methine carbons pointing "up" (+) from methylene and quaternary carbons pointing "down" (-) [14]. IR spectra were recorded with a Bruker Alpha FT-IR spectrometer equipped with an universal ATR sampling accessory. The bond vibration frequencies are expressed in reciprocal centimeters (cm^{-1}). HPLC-MS analyses were performed on a Thermo-Dionex Ultimate 3000 instrument (pump + autosampler at 20 °C + column oven at 25 °C) equipped with a DAD (Thermo-Dionex DAD 3000-RS) and a MSQ Plus single quadrupole mass spectrometer. HPLC-fluorescence analyses were performed with the same instrument but connected to Thermo Scientific Dionex UltiMate 3000 fluorescence detector FLD-3400 RS dual-PMT. UHPLC analyses (implemented during *in vitro* assays with rat liver microsomes) were performed on a Waters Acquity UPLC (H class)/QDa quadrupole MS analyzer (Waters). Purifications by semi-preparative HPLC were performed on a Thermo-Dionex Ultimate 3000 instrument (semi-preparative pump HPG-3200BX) equipped with a RS Variable Detector (VWD-3400RS, four distinct wavelengths within the range 190-800 nm). Lyophilization operations were performed with a Christ Alpha 2-4 LD plus. TFA mass content of samples purified by semi-preparative was determined by ion chromatography according to a method developed by the PACMSUB staff. Such analyses were performed with an ion chromatograph Thermo Scientific Dionex ICS 5000 equipped with a conductivity detector CD (Thermo

Scientific Dionex) and a conductivity suppressor ASRS-ultra II 4 mm (Thermo Scientific Dionex). Low-resolution mass spectra (LRMS) were recorded either on a Thermo Scientific MSQ Plus single quadrupole equipped with an electrospray (ESI) source (LC-MS coupling mode), or on a Bruker Amazon SL instrument equipped with an ESI source (direct introduction mode).

2.3. Synthesis of symmetrical 3,6-bis-(4'-pyridyl)-DPP dye **13** and related NTR-sensitive probe **6**

2.3.1 Di-*tert*-butyl 3,6-bis-(4'-pyridyl)-DPP *N,N'*-diacetate **12**

A suspension of 3,6-Bis-(4'-pyridyl)-DPP pigment **4** (0.255 g, 0.88 mmol, 1.0 equiv.) and *t*BuOK (247 mg, 2.2 mmol, 2.5 equiv.) in dry NMP (20 mL) was stirred at 75 °C under Ar atmosphere for 15 min (color changes from dark pink to night blue). Thereafter, *tert*-butyl bromoacetate (386 μ L, 2.61 mmol, 3 equiv.) was added and the resulting reaction mixture was stirred at 75°C for 90 min (color changes from blue to brown). The reaction was checked for completion by TLC (DCM-EtOAc 8:2, v/v + 1% TEA) and RP-HPLC (system A). After cooling to RT, toluene (60 mL) was added and the resulting organic layer was washed with deionized water (2 \times 100 mL) to remove NMP, dried over anhydrous Na₂SO₄ and finally evaporated to dryness. The resulting residue was purified by column chromatography over silica gel (VWR, technical grade, 40-63 μ m, #84814.360, eluent: step gradient of EtOAc in DCM (+1% TEA) from 0% to 7.5%). Fractions containing the desired product, were combined, washed with aq. 1.0 M KHSO₄ (100 mL) and deionized water (2 \times 100 mL) to remove TEA, dried over anhydrous Na₂SO₄ and evaporated under reduced pressure. Compound **12** was obtained as an orange-brown solid (160 mg, 0.31 mmol, yield 35%). ¹H NMR (600 MHz, CDCl₃): δ = 8.78 (d, ³J_{H-H} = 4.2 Hz, 4H), 7.61 (d, ³J_{H-H} = 5.4 Hz, 4H), 4.39 (s, 4H), 1.36 (s, 18H); ¹³C NMR (150 MHz, CDCl₃): δ = 167.1 (2C), 161.6 (2C), 151.0 (4C), 146.7 (2C), 135.0 (C), 122.1 (4C), 111.4 (2C), 83.5 (C), 44.2 (2C), 28.1 (6C); HPLC (system A): t_R = 4.7 min (purity 99% at 500 nm); UV-vis (recorded during RP-HPLC analysis): λ_{max} = 230, 260 and 477 nm LRMS (ESI+, recorded during RP-HPLC analysis): m/z = 519.2 [M + H]⁺, calcd for C₂₈H₃₁N₄O₆⁺ 519.2.

2.3.2 3,6-Bis-(4'-pyridyl)-DPP *N,N'*-diacetic acid **13**

Di-*tert*-butyl ester **12** (17.0 mg, 32.8 μ mol, 1.0 equiv.) was dissolved in a TFA-DCM (1:1, v/v) mixture (2 mL) and the mixture was stirred at RT for 3 h. The reaction was checked for

completion by RP-HPLC (system B) and the reaction mixture was evaporated to dryness. The resulting residue was dissolved in a (1:1, v/v) mixture of 0.1% aq. TFA and MeCN (4 mL) and purified by semi-preparative RP-HPLC (system C, 1 injection, t_R = 15.8-17.4 min of collected fractions containing the desired compound). The product-containing fractions were lyophilized to give **13** as TFA salt (6.4 mg, 11.3 μ mol, yield 34% based on mass percentage of TFA = 28% determined by ionic chromatography, 1.4 TFA). ^1H NMR (600 MHz, DMSO- d_6): δ = 8.85 (m, 4H), 7.77 (m, 4H), 4.53 (s, 4H); ^{13}C NMR (151 MHz, DMSO- d_6): δ = 170.0 (2C), 161.3 (2C), 150.9 (4C), 146.9 (2C), 134.9 (2C), 122.5 (4C), 110.5 (2C), 43.5 (2C); ^{19}F NMR (565 MHz, DMSO- d_6): δ = -74.5 (3F, CF_3 -trifluoroacetate); HPLC (system B): t_R = 4.3 min (purity 94% at 270 nm and 95% at 500 nm); LRMS (ESI+, recorded during RP-HPLC analysis): m/z 407.3 $[\text{M} + \text{H}]^+$, calcd for $\text{C}_{20}\text{H}_{15}\text{N}_4\text{O}_6^+$ 407.1. *Please note: the poor quality of NMR spectra of this DPP dye was explained by the presence of a further set of signals assigned to the open-chain lactam form **13-RO** formed during the freeze-drying process.* ^1H NMR (600 MHz, DMSO- d_6): δ = 10.26 (bs, 1H, CO_2H), 8.84 (m, 2H), 8.66 (d, J = 5.4 Hz, 2H), 7.83 (d, J = 5.4 Hz, 2H), 7.72 (d, J = 5.4 Hz, 2H), 4.12 (s, 2H), 3.75 (s, 2H); HPLC (system B): t_R = 1.0 min; UV-vis (recorded during RP-HPLC analysis): λ_{max} = 260 and 456 nm; LRMS (ESI+, recorded during RP-HPLC analysis): m/z 425.3 $[\text{M} + \text{H}]^+$, calcd for $\text{C}_{20}\text{H}_{17}\text{N}_4\text{O}_7^+$ 425.1; LRMS (ESI-, recorded during RP-HPLC analysis): m/z 423.2 $[\text{M} + \text{H}]^-$, calcd for $\text{C}_{20}\text{H}_{15}\text{N}_4\text{O}_7^-$ 423.1.

2.3.3. Open-chain lactam form of probe **14**

Di-*tert*-butyl ester **12** (16.8 mg, 32.4 μ mol, 1.0 equiv.) was dissolved in dry MeCN (3 mL), 4-nitrobenzyl bromide (54 mg, 250 μ mol, 7.7 equiv.) was added and the resulting reaction mixture was stirred under reflux and Ar atmosphere for 24 h. The progress of the reaction was checked by RP-HPLC (system B). Thereafter, the reaction mixture was evaporated to dryness. The resulting residue was dissolved in a TFA-DCM (1:1, v/v) mixture (2 mL) and stirred at RT for 3 h. The reaction was checked for completion by RP-HPLC (system A) and the mixture was evaporated to dryness. The resulting residue was dissolved in a (1:1, v/v) mixture of 0.1% aq. TFA and MeCN (4 mL) and purified by semi-preparative RP-HPLC (system C, 1 injection, t_R = 24.5-28.5 min of collected fractions containing the desired compound). The product-containing fractions were lyophilized to give **14** as TFA salt (5.2 mg, 5.6 μ mol, yield 17% based on mass percentage of TFA = 23% determined by ionic chromatography, 1.9 TFA). ^1H NMR (500 MHz, DMSO- d_6): δ = 10.18 (t, $^3J_{\text{H-H}}$ = 5.7 Hz, 1H), 9.15 (d, $^3J_{\text{H-H}}$ = 6.8 Hz, 2H), 8.82 (d, $^3J_{\text{H-H}}$ = 7.1 Hz, 2H), 8.33 (m, 4H), 8.07 (d, $^3J_{\text{H-H}}$ = 6.8 Hz, 2H), 7.88 (d, $^3J_{\text{H-H}}$ = 7.1 Hz, 2H),

7.82 (d, $^3J_{\text{H-H}} = 8.8$ Hz, 2H), 7.76 (d, $^3J_{\text{H-H}} = 8.8$ Hz, 2H), 6.02 (s, 2H), 5.83 (s, 2H), 4.20 (s, 2H), 3.82 (d, $^3J_{\text{H-H}} = 5.7$ Hz, 2H); ^{13}C NMR (151 MHz, DMSO- d_6): $\delta = 178.7, 171.3, 170.6, 166.0, 164.7, 159.2, 148.0, 147.9, 147.7, 144.6, 142.8, 141.6, 141.3, 134.9, 134.8, 130.2$ (2C), 129.9 (2C), 129.6, 127.0, 126.7, 125.7, 125.4, 124.4 (2C), 124.3 (2C), 124.2, 123.8, 123.3, 121.2, 101.8, 62.0, 61.7, 60.7, 42.5, 41.1, 36.5, 16.9; HPLC (system A): $t_{\text{R}} = 3.1$ min (purity 88% at 270 nm and 98% at 500 nm); LRMS (ESI+, recorded during RP-HPLC analysis): m/z 695.2 [$\text{M}^{2+} - \text{H}$] $^+$, calcd for $\text{C}_{34}\text{H}_{27}\text{N}_6\text{O}_{11}^+$ 695.2; LRMS (ESI-, recorded during RP-HPLC analysis): m/z 693.2 [$\text{M} - 3\text{H}$] $^-$, calcd for $\text{C}_{34}\text{H}_{25}\text{N}_6\text{O}_{11}$ 693.2.

2.4. Synthesis of unsymmetrical mono-(4'-pyridyl)-DPP dye **17** and related NTR-sensitive probe **7**

2.4.1 Di-*tert*-butyl mono-(4'-pyridyl)-DPP *N,N'*-diacetate **16**

A suspension of mono-(4'-pyridyl)-DPP pigment **5** (250 mg, 0.68 mmol, 1.0 equiv.) and *t*BuOK (190 mg, 1.70 mmol, 2.5 equiv.) in dry NMP (30 mL) was stirred at 75 °C under N_2 atmosphere for 15 min. *tert*-Butyl bromoacetate (300 μL , 2.04 mmol, 3.0 equiv) was added and the mixture was stirred at 75 °C under N_2 for 90 min. Thereafter, the mixture was cooled down to RT and deionized water was added. The product was extracted with toluene three times. The combined organic layers were dried over anhydrous Na_2SO_4 , filtered and the solvent was evaporated under reduced pressure. The product was purified by column chromatography over silica gel (VWR technical grade, 40-63 μm , #84814.360) using a step gradient of EtOAc in DCM as eluent (from 0% to 10% + 1% TEA). Compound **16** was obtained as an orange solid (86.0 mg, 144 μmol , yield 22%). ^1H NMR (500 MHz, CDCl_3): $\delta = 8.73$ (brs, 2H), 7.76 (brs, 2H), 7.61 (m, 4H), 4.38 (s, 2H), 4.32 (s, 2H), 1.34 (s, 9H), 1.32 (s, 9H); ^{13}C NMR (126 MHz, CDCl_3): $\delta = 167.3, 167.2, 162.0, 161.7, 150.8, 149.2, 144.8, 135.3, 132.6$ (2C), 130.3 (2C), 126.8, 126.4, 122.0, 111.5, 109.9, 83.3, 83.2, 44.3, 44.1, 28.0 (6C); HPLC (system A): $t_{\text{R}} = 5.6$ min (purity 85% at 260 nm and 95% at 470 nm); UV-vis (recorded during RP-HPLC analysis): $\lambda_{\text{max}} = 261, 299$ and 462 nm; LRMS (ESI+, recorded during RP-HPLC analysis): m/z 596.2 and 598.2 [$\text{M} + \text{H}$] $^+$, calcd for $\text{C}_{29}\text{H}_{31}\text{BrN}_3\text{O}_6^+$ 596.1 and 598.1.

2.4.2 Mono-(4'-pyridyl)-DPP *N,N'*-diacetic acid **17**

To a solution of di-*tert*-butyl ester **16** (16.2 mg, 27 μmol , 1.0 equiv) in DCM (2 mL), TFA (2 mL) was added. The mixture was stirred at RT for 4 h. Thereafter, the reaction mixture was evaporated to dryness. The resulting residue was dissolved in a (2:1, v/v) mixture of 0.1% aq.

TFA and MeCN (3 mL) and purified by semi-preparative RP-HPLC (system E, 1 injection, t_R = 35.0-42.5 min of collected fractions containing the desired compound). The product-containing fractions were lyophilized to give TFA salt of **17** as an orange amorphous powder (7.8 mg, 14 μ mol, yield 50% based on mass percentage of TFA = 15% determined by ionic chromatography, 0.7 TFA). ^1H NMR (500 MHz, DMSO- d_6): δ = 13.24 (brs, 2H), 8.83 (d, $^3J_{\text{H-H}}$ = 6.1 Hz, 2H), 7.84 (d, $^3J_{\text{H-H}}$ = 8.5 Hz, 2H), 7.75 (m, 4H), 4.53 (s, 2H), 4.49 (s, 2H); ^{13}C NMR (151 MHz, DMSO- d_6): δ = 170.1, 161.7, 161.3, 151.0, 149.1, 145.2, 134.9, 132.7, 131.0, 126.6, 126.1, 122.4, 110.6, 109.1, 56.5, 43.6, 43.5; ^{19}F NMR (565 MHz, DMSO- d_6): δ = -73.9 (3F, CF_3 -trifluoroacetate), -75.2 (0.19F, CF_3 -free TFA); HPLC (system A): t_R = 3.6 min (purity 94% at 460 nm); UV-vis (recorded during RP-HPLC analysis): λ_{max} = 260, 307 and 475 nm; LRMS (ESI+, recorded during RP-HPLC analysis): m/z 484.1 and 486.1 $[\text{M} + \text{H}]^+$, calcd for $\text{C}_{21}\text{H}_{15}\text{BrN}_3\text{O}_6^+$ 484.0 and 486.0.

2.4.2 *N*-(4-Nitrobenzyl)pyridinium mono-(4'-pyridyl)-DPP *N,N'*-diacetic acid **7**

To a solution of di-*tert*-butyl ester **16** (34 mg, 57 μ mol, 1.0 equiv.) in dry MeCN (5 mL), 4-nitrobenzyl bromide (99 mg, 456 μ mol, 8.0 equiv.) was added. The mixture was refluxed under N_2 atmosphere overnight. Thereafter, the reaction mixture was evaporated to dryness. The resulting residue was dissolved in DCM (2 mL) and TFA (2 mL) was added dropwise. The mixture was stirred at RT for 3 h, then evaporated to dryness. The resulting residue was dissolved in a (2:3, v/v) mixture of 0.1% aq. TFA and MeCN (4 mL) and purified twice by semi-preparative RP-HPLC (system D, 1 injection, t_R = 46.0-50.0 min of collected fractions containing the desired compound). The product-containing fractions were lyophilized to give TFA salt of **7** as a purple solid (4.9 mg, 6.7 μ mol, yield 12% based on mass percentage of TFA = 17% determined by ionic chromatography, 1.1 TFA). ^1H NMR (500 MHz, DMSO- d_6): δ 13.34 (brs, 2H), 9.36 (d, $^3J_{\text{H-H}}$ = 6.5 Hz, 2H), 8.47 (d, $^3J_{\text{H-H}}$ = 6.5 Hz, 2H), 8.33 (d, $^3J_{\text{H-H}}$ = 8.1 Hz, 2H), 7.88 (m, 2H), 7.82 (m, 4H), 6.04 (s, 2H), 4.59 (s, 2H), 4.53 (s, 2H); ^{19}F NMR (565 MHz, DMSO- d_6): δ = -73.5 (3F, CF_3 -TFA); *full spectroscopic characterization of this probe through ^{13}C NMR measurements was not completed immediately, and an unexpected degradation occurring at the solid state has prevented us to record ^{13}C NMR spectrum.* HPLC (system A): t_R = 3.8 min (purity 98% at 260 nm and 100% at 520 nm); UV-vis (recorded during RP-HPLC analysis): λ_{max} = 271, 330 and 518 nm; LRMS (ESI+, recorded during RP-HPLC analysis): m/z 619.2 and 621.2 $[\text{M}]^+$, calcd for $\text{C}_{28}\text{H}_{20}\text{BrN}_4\text{O}_8^+$ 619.1 and 619.2.

2.5. Synthesis of unsymmetrical mono-(4'-pyridyl)-DPP dye **18** and related Azor- and NTR-sensitive probes **8** and **9**

2.5.1 Mono-(4'-pyridyl)-DPP *N,N'*-dimethyl **18**

A suspension of mono-(4'-pyridyl)-DPP pigment **5** (300 mg, 0.81 mmol, 1.0 equiv.) and *t*BuOK (229 mg, 2.04 mmol, 2.5 equiv.) in dry NMP (30 mL) was stirred at RT under nitrogen for 15 min. MeI (151 μ L, 2.44 mmol, 3.0 equiv.) was added and the mixture was stirred at RT under N₂ for 1 h. Deionized H₂O was added and the product was extracted with toluene three times. The combined organic layers were dried over anhydrous Na₂SO₄, filtered and the solvent was evaporated under reduced pressure. Compound **18** was obtained as a dark-orange solid (141 mg, 0.35 mmol, yield 44%). IR (ATR): ν = 3046, 2850, 1650, 1587, 1539, 1494, 1468, 1425, 1397, 1363, 1283, 1218, 1098, 1071, 1045, 1006, 824, 757, 740, 729, 701, 687, 647, 582, 554, 535, 519, 496, 469, 434, 423, 412, 402; ¹H NMR (500 MHz, CDCl₃): δ = 8.90 (d, ³*J*_{H-H} = 5.5 Hz, 2H), 8.11 (d, ³*J*_{H-H} = 5.5 Hz, 2H), 7.84 (d, ³*J*_{H-H} = 8.6 Hz, 2H), 7.75 (d, ³*J*_{H-H} = 8.6 Hz, 2H), 3.44 (s, 3H), 3.39 (s, 3H); ¹³C NMR (126 MHz, CDCl₃): δ = 162.3, 162.0, 150.2 (2C), 149.8, 144.7, 135.5, 132.4 (2C), 130.8 (2C), 126.9, 126.3, 122.5 (2C), 111.4, 109.4, 29.6, 29.5; HPLC (system A): *t*_R = 4.7 min (purity 99% at 260 nm and 100% at 460 nm); UV-vis (recorded during RP-HPLC analysis): λ_{max} = 264 and 485 nm; LRMS (ESI+, recorded during RP-HPLC analysis): *m/z* 396.1 and 398.1 [M + H]⁺, calcd for C₁₉H₁₅BrN₃O₂⁺ 396.0 and 398.0.

2.5.2 *N*-(4-[2-[4-(dimethylamino)phenyl]diazenyl]-benzyl)pyridinium mono-(4'-pyridyl)-DPP *N,N'*-dimethyl **8**

To a solution of **18** (22.0 mg, 56 μ mol, 1.0 equiv.) in dry DMF (5 mL), benzyl bromide **19** (53.0 mg, 167 μ mol, 3.0 equiv.) was added. The resulting mixture was stirred at 75 °C under N₂ for 12 h. Thereafter, this mixture was evaporated under reduced pressure and the resulting residue was purified by column chromatography over silica gel (VWR technical grade, 40-63 μ m, #84814.360, eluent: a step gradient of MeOH in DCM as eluent from 5% to 15%). The isolated product was dissolved in a (1:3, v/v) mixture of 0.1% aq. TFA and MeCN and (4 mL) and subjected to a further purification by semi-preparative RP-HPLC (system F, 1 injection, *t*_R = 55.0-63.0 min of collected fractions containing the desired compound). The product-containing fractions were lyophilized to give TFA salt of **8** as a purple solid (7.9 mg, 9.5 μ mol, yield 17% based on mass percentage of TFA = 24% determined by ionic chromatography, 1.8 TFA). IR (ATR): ν 2923, 1674, 1629, 1599, 1519, 1488, 1429, 1365, 1200, 1136, 1073, 1043, 1005, 943, 830, 798, 756, 720, 687, 639, 600, 583, 553, 511, 496, 469, 434, 413; ¹H NMR (500 MHz,

CDCl₃): δ = 9.20 (d, $^3J_{H-H}$ = 6.4 Hz, 2H), 8.57 (d, $^3J_{H-H}$ = 6.4 Hz, 2H), 7.89 (m, 4H), 7.81 (d, $^3J_{H-H}$ = 8.7 Hz, 2H), 7.70 (d, $^3J_{H-H}$ = 8.7 Hz, 2H), 7.62 (d, $^3J_{H-H}$ = 8.2 Hz, 2H), 6.75 (d, $^3J_{H-H}$ = 9.2 Hz, 2H), 6.02 (s, 2H), 3.48 (s, 3H), 3.36 (s, 3H), 3.11 (s, 6H); ¹³C NMR (151 MHz, CD₃CN): δ 162.1, 161.1, 153.9, 153.3, 153.3, 144.7, 143.1, 143.0, 139.3, 133.4, 132.2, 131.3, 130.4, = 126.8, 126.5, 126.1, 125.1, 122.7, 115.5, 111.6, 109.7, 63.9, 39.5, 29.2, 29.1; ¹⁹F NMR (565 MHz, CD₃CN) δ = -75.9 (3F, CF₃-trifluoroacetate), -76.5 (0.05F, CF₃-free TFA); HPLC (system A): t_R = 4.9 min (purity 97% at 260 and 98% at 460 nm); UV-vis (recorded during RP-HPLC analysis): λ_{max} = 280 and 452 nm; LRMS (ESI+, recorded during RP-HPLC analysis): m/z 633.4 and 635.4 [M]⁺, calcd for C₃₄H₃₀BrN₆O₂⁺ 633.2 and 635.2.

2.5.3 *N*-(4-Nitrobenzyl)pyridinium mono-(4'-pyridyl)-DPP *N,N'*-dimethyl **9**

To a solution of **18** (20.0 mg, 51 μ mol, 1.0 equiv.) in dry MeCN (3 mL) was added 4-nitrobenzyl bromide (32.7 mg, 150 μ mol, 2.9 equiv.). The resulting reaction mixture was stirred at 75 °C under N₂ overnight and the disappearance of the starting material was checked by RP-HPLC (system A). Thereafter, the mixture was evaporated under reduced pressure, re-dissolved in a (1:3, v/v) mixture of 0.1 % aq. TFA and MeCN (4 mL) and purified by semi-preparative RP-HPLC (system F, 1 injection, t_R = 43.0-50.0 min of collected fractions containing the desired compound). The product-containing fractions were lyophilized to give TFA salt of **9** as a purple solid (8.3 mg, 12 μ mol, yield 24% based on mass percentage of TFA = 22% determined by ionic chromatography, 1.3 TFA). IR (ATR): ν = 3046, 2923, 1670, 1630, 1564, 1520, 1487, 1430, 1402, 1374, 1347, 1289, 1197, 1165, 1125, 1072, 1043, 1005, 830, 798, 759, 736, 718, 705, 686, 619, 521, 489, 441, 411; ¹H NMR (500 MHz, CD₃CN): δ = 8.84 (d, J = 7.1 Hz, 2H), 8.54 (d, J = 7.1 Hz, 2H), 8.30 (d, J = 8.8 Hz, 2H), 7.92 (d, J = 8.7 Hz, 2H), 7.80 (d, J = 8.7 Hz, 2H), 7.69 (d, J = 8.8 Hz, 2H), 5.85 (s, 2H), 3.37 (s, 3H), 3.30 (s, 3H); ¹³C NMR (126 MHz, CD₃CN): δ = 162.9, 161.8, 154.2, 145.8, 144.0, 140.3, 139.9, 133.0, 132.1, 131.1, 127.6, 127.4, 126.8, 125.1, 63.7, 29.9, 29.9; ¹⁹F NMR (565 MHz, CD₃CN): δ = -75.5 (3F, CF₃-trifluoroacetate; HPLC (system A): t_R = 3.4 min (purity 99% at 260 nm, 98 % at 460 nm and 100% at 520 nm); UV-vis (recorded during RP-HPLC analysis): λ_{max} = 264 and 539 nm; LRMS (ESI+, recorded during RP-HPLC analysis): m/z 531.2 and 533.3 [M]⁺, calcd for C₂₆H₂₀BrN₄O₄⁺ 531.1 and 533.1.

2.6. Synthesis of PGA-sensitive probe **10** based on unsymmetrical mono-(4'-pyridyl)-DPP **18**

To a solution of **18** (20.0 mg, 51 μ mol, 1.0 equiv.) in dry MeCN (5 mL) was added benzyl bromide **20** (46.0 mg, 150 μ mol, 2.9 equiv.). The resulting reaction mixture was stirred at 75 °C under N₂ for 12 h. The disappearance of the starting material was checked by RP-HPLC (system A) and the mixture was evaporated under reduced pressure. The residue was dissolved in a (1:3, v/v) mixture of 0.1 % aq. TFA and MeCN (4 mL) and purified by semi-preparative RP-HPLC (system F, 1 injection, t_R = 47.5-55.5 min of collected fractions containing the desired compound). The product-containing fractions were lyophilized to give TFA salt of **10** as a purple solid (9.7 mg, 12.4 μ mol, yield 25 % based on mass percentage of TFA = 20% determined by ionic chromatography, 1.4 TFA). IR (ATR): ν = 1672, 1631, 1602, 1537, 1515, 1488, 1416, 1373, 1199, 1131, 1073, 1044, 1006, 833, 798, 755, 719, 625, 517, 433, 412; ¹H NMR (500 MHz, CD₃CN): δ = 8.91 (s, 1H), 8.78 (d, J = 7.1 Hz, 2H), 8.46 (d, J = 7.1 Hz, 2H), 7.90 (d, J = 8.7 Hz, 2H), 7.79 (d, J = 8.6 Hz, 2H), 7.70 (d, J = 8.7 Hz, 2H), 7.44 (d, J = 8.6 Hz, 2H), 7.38-7.29 (m, 4H), 7.28-7.24 (m, 1H), 5.66 (s, 2H), 3.67 (s, 2H), 3.33 (s, 3H), 3.28 (s, 3H); ¹³C NMR (126 MHz, CD₃CN): δ = 170.8, 163.0, 162.1, 154.1, 145.5, 143.8, 141.6, 140.3, 136.6, 133.1, 132.3, 131.2, 130.2, 129.4, 128.4, 127.8, 127.7, 127.4, 127.1, 121.0, 110.6, 64.8, 44.5, 30.1, 30.0; ¹⁹F NMR (565 MHz, CD₃CN): δ = -76.0 (3F, CF₃-trifluoroacetate); HPLC (system A): t_R = 3.5 min (purity 97% at 260 nm and 100% at 460 nm); UV-vis (recorded during RP-HPLC analysis): λ_{max} = 256 and 534 nm; LRMS (ESI+, recorded during RP-HPLC analysis): m/z 619.3 and 621.3 [M]⁺, calcd for C₃₄H₂₈BrN₄O₃⁺ 619.1 and 621.1.

2.7 *In vitro* activation of DPP-based probes **7-11** by PGA or reductases - experimental details

2.7.1 Stock solutions of fluorogenic probes, enzymes and co-factor (NADH)

Stock solutions of DPP-based fluorogenic probes (1.0 mg/mL) were prepared in DMSO (spectrophotometry grade). Solution NTR was prepared by dissolving the commercial lyophilized powder in ultrapure water (0.1 U/ μ L). Stock solution of NADH (140 mM) was prepared from commercial powder and ultrapure water. Commercial PGA solution (841 U/mL) was directly used without dilution. Solution of LAP was prepared by dissolving 14.2 μ L of the commercial suspension in 985.8 μ L of ultrapure water (0.001 U/ μ L). *Please note*: stock solutions of parent DPP fluorophores were also prepared in DMSO (1.0 mg/mL) but prolonged sonication is required to completely solubilize *N,N'*-dimethyl DPP dye in this polar aprotic solvent.

2.7.2 Fluorescence-based assays

All assays were performed at 37 °C (using a temperature control system combined with water circulation and conducted with magnetic stirring). For all probes **7-11** (final concentration in 3.5 mL fluorescence quartz cell: 1.0 μM, volume: 3.0 mL of PB, pH 7.6), the fluorescence emission of the released mono-(4'-pyridyl)-DPP dye was monitored at $\lambda(\text{Ex./Em.}) = 440/555$ nm = 5 nm, over time with measurements recorded every 5 s. For assays conducted with NTR/NADH, 1 μL of co-factor solution (final concentration in quartz cell: 47 μM) was added after 5 min of incubation of the probe in PB, and NTR (1 μL, 0.1 U) after 5 min of incubation with NADH. For assays conducted with amidase/peptidase, 1.2 μL of PGA solution (1 U) or 2 μL of LAP solution (0.002 U) was added after 5 min of incubation of the probe in PB. Blank experiments to assess the stability of the probes in PB, were achieved in the same way but without adding the corresponding enzyme. Further blank experiments were performed with PGA-sensitive probe **10**, either under Ar atmosphere (bubbling of Ar for 15 min prior to incubation in PB, use of a quartz cell with screw top, sealing cap, Starna Scientific, #3-Q-10-GL14-C, to keep such Ar atmosphere), or in the presence of NaN₃ (final concentration: 14.3 mM), or in acetate buffer (0.1 M, pH 5.6).

2.7.3 RP-HPLC-fluorescence and RP-HPLC-MS (full scan and SIM modes) analyses

Enzymatic reaction mixtures from fluorescence-based *in vitro* assays were directly analyzed by RP-HPLC-fluorescence after an incubation time of 60-150 min (injected volume: 20 μL, system H). Thereafter, each enzymatic reaction mixture (ca. 3 mL) was freeze-dried; the resulting white amorphous powder was dissolved in a (1:1, v/v) mixture of ultrapure H₂O and MeCN (total volume = 400-1000 μL depending on the kinetics). The solution was vortexed followed by centrifugation (9 000 rpm, 1 min). 20 μL of supernatant was injected into the HPLC-MS apparatus (system I). *Please note: injection of PB and H₂O-MeCN (1:1, v/v) were also achieved immediately prior to this latter analysis, especially to confirm the lack of residual contaminants within the C₁₈ column or ESI probe at the corresponding m/z value selected for the SIM detection mode and then avoid misinterpretations.* For RP-HPLC (fluorescence or MS detection) analyses of mono-(4'-pyridyl)-DPP samples, 1.0 μM solution in PB was prepared and 20 μL was injected into the HPLC-fluorescence/MS apparatus (systems H and I).

2.7.4 *In vitro* assays with rat liver microsomes

All animal experiments were conducted in accordance with institutional guidelines. Rats (Wistar, ♂ 6-7 weeks) were purchased from CLEA Japan company. Rats were fasted overnight

and sacrificed by exsanguination from the abdominal aorta. The liver containing 0.15 M KCl (pH 7.4) was homogenized in 3 volumes of the same buffer. Microsomes were prepared according to the method of Omura and Sato [15]. Microsomes contained 51.0 mg protein/mL and 0.82 nmol P450/mg protein. They were diluted with 0.1 M potassium phosphate buffer at pH 7.4 for assay and the final concentration was 170 $\mu\text{g/mL}$. Azo-based fluorogenic probes **8** and **MAR** (1.0 μM) were incubated in the presence of rat liver microsomes (*vide supra*) under hypoxic conditions. Fluorescence measurements were performed in PB (0.1 M, pH 7.4) containing DMSO (0.1%) as a co-solvent and the enzymatic reaction mixtures were also subjected to UHPLC analyses (see Fig. S88-S94 for more details). NADPH (50 μM) was added after 5 min. The hypoxic conditions were prepared by bubbling Ar gas into the reaction solution for 30 min.

3. Results and discussion

In order to simplify the synthesis of fluorogenic pyridyl-based DPP dyes, and contrary to the structure intensively studied by the Hua group [7], we have chosen to focus first on the preparation of a symmetrical derivative based on the easily-accessible 3,6-bis(4'-pyridyl)-DPP dye, equipped with two identical enzyme-recognition moieties and hence operating as a dual-reactable probe. Due to the prominent role of reductases (*i.e.*, AzoR, NTR and quinone-reductases such as DT-diaphorase) in devising optical detection/imaging methods of tumor hypoxia (*i.e.*, oxygen-deprivation state) [16] and bacterial infections [17], we selected the well-known NTR-4-nitrobenzyl pair for rapid access to DPP-based fluorogenic enzyme substrates and to facilitate *in vitro* validations of their fluorogenicity. To improve aq. solubility of the overall structure while keeping a neutral state at physiological pH, the introduction of carboxymethyl arms through *N*-lactam alkylation has been also considered.

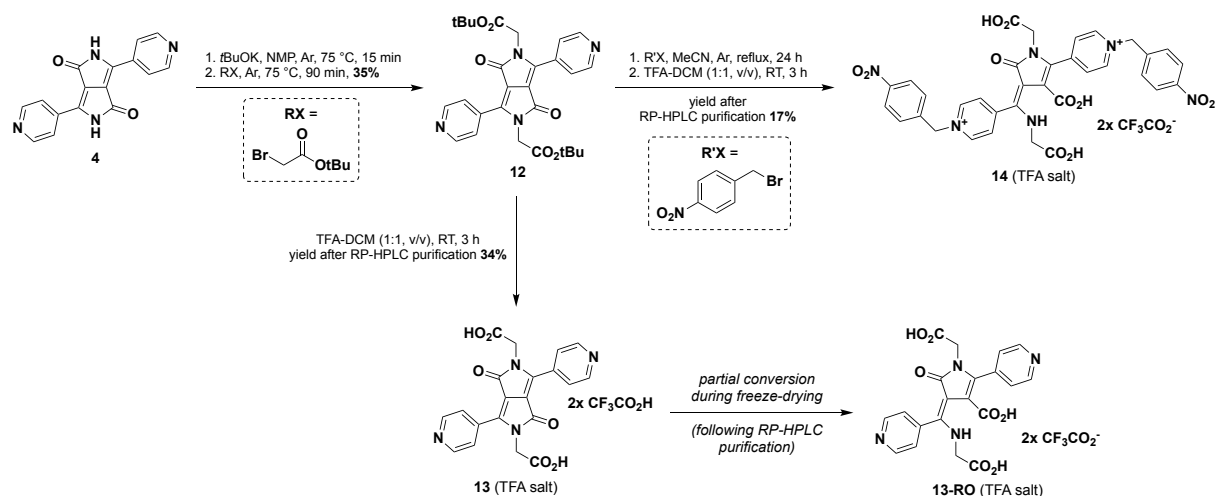
3.1 Synthesis and aqueous stability of NTR-sensitive probe **6** based on symmetrical 3,6-bis-(4'-pyridyl)-DPP

As displayed in Scheme 1, the planned synthetic route towards the water-soluble NTR-sensitive probe **6** was based on the sequential *N*-alkylation of lactam and pyridyl moieties of 3,6-bis-(4'-pyridyl)-DPP **4** with *tert*-butyl bromoacetate and 4-nitrobenzyl bromide

respectively. As we had anticipated, the main difficulty associated with this synthesis was the selective *N*-substitution of lactam units with the protected carboxymethyl arm. On the basis of the valuable work of Vakuliuk *et al.* [18] identifying *t*BuOK as the most suited base to promote this challenging *N*-alkylation and by conducting a rapid screening of reaction conditions (solvent, heating temperature and duration), we have managed to optimize this step and the corresponding *N,N'*-dialkyl-DPP **12** was obtained in an acceptable 35% yield after purification by column chromatography over silica gel. Thereafter, quaternization of pyridyl moieties with 4-nitrobenzyl bromide was readily achieved by treatment of **12** with a large excess of this alkylating agent (7.7 equiv.) in refluxing MeCN for 24 h. It is important to specify that the addition of an inorganic base such as K₂CO₃, in an attempt to accelerate this reaction, has led to rapid and complete degradation of the bis-lactam-fused structure. Fully *N*-alkylated crude product was directly subjected to anhydrous acidic conditions TFA-DCM (1:1, v/v) for the deprotection of *t*Bu esters, and to obtain the targeted water-soluble fluorogenic probe **6**. Unfortunately, all our attempts to isolate this highly polar compound by semi-preparative RP-HPLC (different aq. mobile phases with pH in the range 2.0-6.0) failed owing to its instantaneous conversion into the mono-lactam ring-opening product **14**. Its structure was confirmed by detailed measurements including ESI mass spectrometry and NMR analyses (see supporting information for the corresponding spectra, Figs. S51-S56). To the best of our knowledge, this propensity to undergo lactam hydrolysis under acidic or neutral aq. conditions, has never been reported for DPP dyes. One possible explanation may be the strong electron-withdrawing effect of both *N*-(4-nitrobenzyl) pyridinium moieties that dramatically enhance electrophilicity of lactam carbonyl and hence its facile reaction with water molecules. This hypothesis is strengthened by the fact that the parent DPP fluorophore **13** bearing free pyridyl nitrogen positions, synthesized according the same overall strategy (Scheme 1), was found to be a more stable and isolatable compound. However, we noted that the acidic conditions used for its RP-HPLC purification favored its partial conversion (during the freeze-drying process) into the corresponding non-fluorescent ring-opened derivative **13-RO**.

This unexpected result allows us to unambiguously state that 3,6-bis-(4'-pyridyl)-DPP **4** is not a suitable photoactive platform to construct reaction-based fluorescent probes for use in aq. environments, whose modulation of output optical signal is based on a *N*-pyridyl alkylation-dealkylation process. Perhaps as a result, the Hua group preferred to use an unsymmetrical analog bearing a single fluorogenic 4-pyridyl group for designing esterase- and γ -GT-activated

ratiometric probes **1** and **3** [7a, 7c]. Thus, we have been focused on this type of DPP pigments for our next investigations.

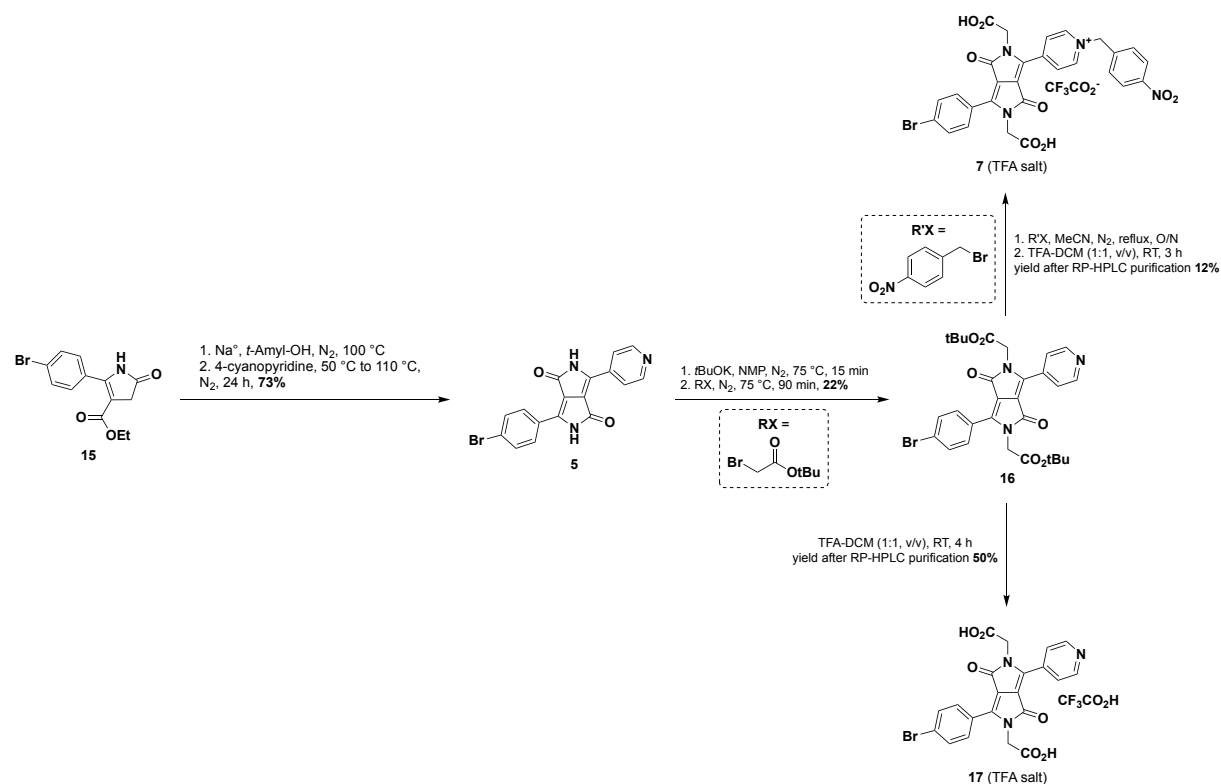


Scheme 1. Synthesis of water-soluble 3,6-bis-(4'-pyridyl)-DPP dye **13** and open-chain lactam form **14** of targeted NTR-sensitive fluorogenic probe **6** (Ar = argon, NMP = *N*-methyl-2-pyrrolidone, RT = room temperature).

3.2 Synthesis of AzoR- and NTR-sensitive probes based on unsymmetrical mono-(4'-pyridyl)-DPP

The synthetic route towards the unsymmetrical analog of NTR-sensitive probe discussed above, is very similar to that depicted in Scheme 1. The key step was the preparation of mono-(4'-pyridyl)-DPP pigment **5** through a two-step procedure based on literature protocols (Scheme 2 and supporting information). Contrary to the DPP structure selected by the Hua group [7a, 7c], we have chosen to work with a pigment bearing the 4-bromophenyl moiety as the second (hetero)aryl substituent. Indeed, the availability of a reactive bromine atom will enable a further functionalization of the probe, through post-synthetic Pd-catalyzed derivatization, if structural elements (and properties associated with) are specifically required for a particular biosensing/bioimaging application. Briefly, 3-ethoxycarbonyl-2-pyrrolin-5-one **15** carrying 4-bromophenyl substituent was reacted with 4-cyanopyridine in the presence of sodium *tert*-amylate (*t*-AmylONa, *in situ* generation through reaction of *tert*-amyl alcohol with metallic sodium) to give DPP pigment **5** in a satisfying 73% yield. This compound was undergone the *N*-alkylation/pyridine quaternization/*t*Bu ester deprotection sequence to give the NTR-sensitive probe. Purification was achieved by semi-preparative RP-HPLC under acidic conditions (*i.e.*, linear gradient of MeCN in aq. TFA 0.1%, pH 2.0) that enabled isolation of **7** (TFA salt) in a pure form (>95%) required for photophysical studies and enzymatic bioassays. In order to have

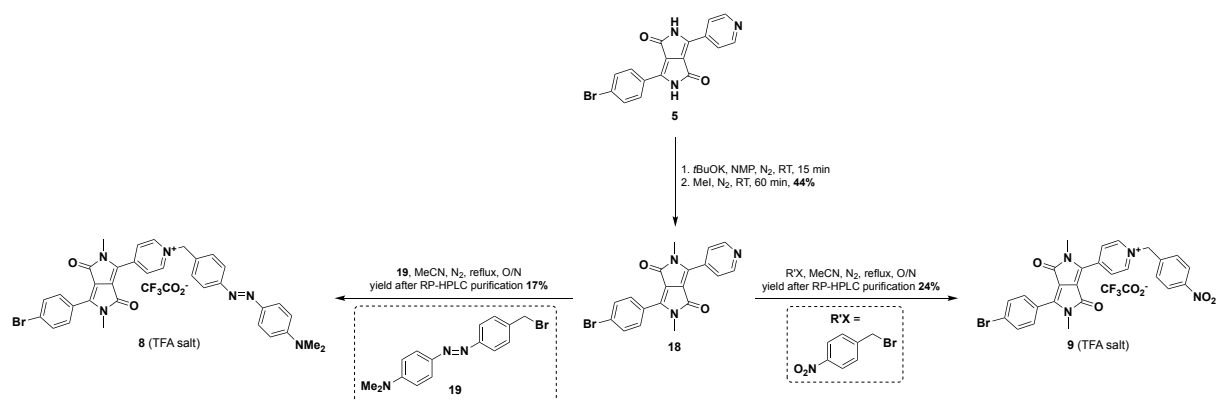
the reference for fluorescence assays and HPLC analyses (see subsections 3.4 and 3.5), the parent DPP fluorophore **17** was prepared using the same reaction sequence whilst omitting quaternization of pyridyl moiety with 4-nitrobenzyl bromide.



Scheme 2. Synthesis of water-soluble mono-(4'-pyridyl)-DPP dye **17** and related NTR-sensitive fluorogenic probe **7** (*t*-AmylOH = *tert*-amyl alcohol or 2-methylbutano-2-ol, NMP = *N*-methyl-2-pyrrolidone, O/N = overnight, RT = room temperature).

To expand the range of hypoxia-related reductases detectable with fluorogenic pyridine-flanked DPP platform **5**, a second bioreductive recognition moiety, sensitive to AzoR activity, was also considered. Installation of a self-immolative azobenzene was achieved using 4-[2-[4-(dimethylamino)phenyl]diazenyl]-benzyl bromide **19** as alkylating agent (see supporting information for its synthesis) and under the same conditions previously used for the reactions conducted with 4-nitrobenzyl bromide. Another structural change has been made and has concerned *N*-lactam substituents. Indeed, the methyl group was preferred to the carboxymethyl moiety in order to obtain a positively-charged compound more suited to biological models possibly contemplated to validate fluorogenic activation by AzoR. Indeed, contrary to NTRs, some of which are commercially available and easy to use in the context of *in vitro* enzyme assays (*e.g.*, recombinant NTR expressed in *E. coli*), isolated forms of AzoR are not readily available. Synthetic reactions for the preparation of AzoR-sensitive probe **8** and its parent fluorophore **18** are summarized in Scheme 3. Their purification was achieved by semi-preparative RP-HPLC. The NTR-sensitive probe **9** based on the same fluorogenic *N,N'*-

dimethyl-DPP dye was also prepared using a similar synthetic route, to allow a comprehensive and relevant comparison in terms of enzymatic reactivity. All spectroscopic data (see supporting information for the corresponding spectra, Figs. S1-S5, S8-S14, S16-S22, S60-S65 and S67-S72), especially NMR and ESI mass spectrometry, were in agreement with the five structures assigned. The purity of **7-9**, **17** and **18** was confirmed by RP-HPLC analysis with UV-vis detection at different wavelengths, and mass percentage of TFA was determined by ionic chromatography (see supporting information, Figs. S6, S15, S23 and S66).



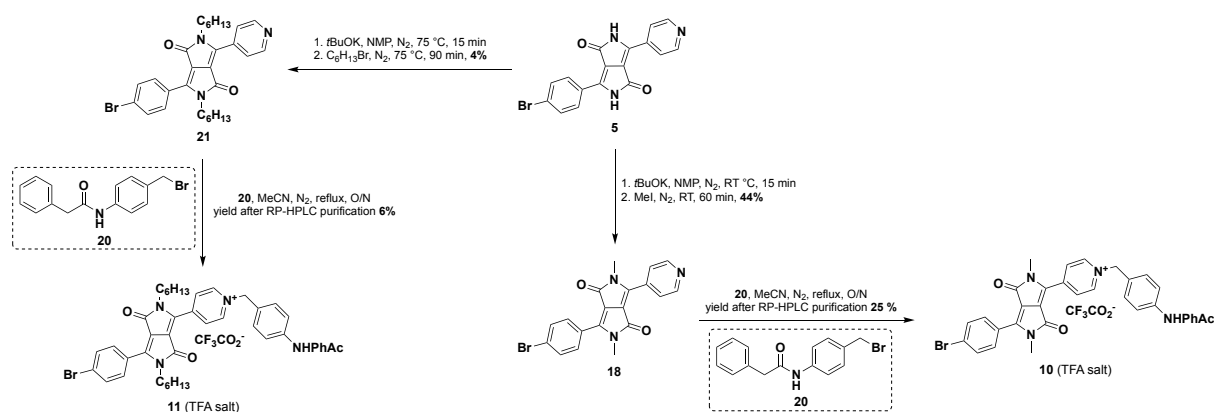
Scheme 3. Synthesis of *N,N'*-dimethyl-DPP dye **18** and related AzoR- and NTR-sensitive fluorogenic probes **8** and **9** (NMP = *N*-methyl-2-pyrrolidone, O/N = overnight).

3.3 Synthesis of PGA-sensitive probes based on unsymmetrical mono-(4'-pyridyl)-DPP

Due to its many positive attributes including commercial availability at a reasonable cost, stability especially under an immobilized form and structurally simple substrate (phenylacetyl moiety, PhAc), penicillin G acylase (PGA) is widely used as biocatalyst in the synthesis of β -lactam antibiotics [19], for kinetic resolution of racemates and as reagent for the removal of PhAc-based protecting groups. PGA is often regarded as a valuable model protease to perform *in vitro* validations of self-immolative molecular systems used as diagnostic probes, molecular amplifiers or drug delivery systems [20]. Furthermore, several fluorescent probes were recently developed to image endogenous bacterial PGA and thus help microbial diagnostics both in health area and food industry [21]. Thus, there is a real interest for the development of novel fluorogenic PGA substrates with superior performances.

As illustrated by numerous examples documented in the literature, the most universal and frequently used PGA-sensitive triggering unit is *para*-(phenylacetamido)benzyl moiety which is readily introduced through a carbamate or an ether linkage depending on the nature and reactivity of optically tunable group to be masked [20],[22]. In the present case, the availability

of *N*-alkylating agent *para*-(phenylacetamido)benzyl bromide **20** (see supporting information for its optimized synthesis) has enabled us to use again the synthetic route initially devised for the two other probes based on *N,N'*-dimethyl DPP **18**, and hence to easily obtain the targeted compound **10** (Scheme 4).



Scheme 4. Synthesis of PGA-sensitive fluorogenic probes **10** and **11** and *N,N'*-dihexyl-DPP dye **21** (NMP = *N*-methyl-2-pyrrolidone, O/N = overnight).

Finally, to facilitate comparison with results obtained by the Hua group [7a, 7c], we have also prepared the analog **11** for which the fluorogenic DPP platform is *N,N'*-substituted by hexyl moieties, even if we were highly sceptical about the relevance of this choice done for the construction of their esterase- and γ -GT-activated ratiometric probes **4** and **6**, intended to be used in aq. media. As was the case for reductase-sensitive probes, the structure of each fluorogenic PGA substrate was confirmed by detailed spectroscopic measurements including NMR and ESI-MS analyses (see supporting information for the corresponding spectra, Figs. S25-S39 and S80-S85).

3.4 Photophysical behavior of enzyme-sensitive DPP-based probes and parent fluorophores

The spectral properties of the novel pyridine-flanked DPP fluorophores and the related enzyme-sensitive DPP-based probes were evaluated and collected parameters are summarized in Table 1 (see Figs. 2 and 3 for the absorption/fluorescence spectra of **8**, **10**, **13**, **17** and **18**, and Figs. S7, S24, S40-S41, S86-S87 for **7**, **9**, **11** and **21**). In contrast to photophysical characterizations performed by the Hua group on DPP derivatives **1-3**, we have deliberately chosen phosphate buffer (PB, 0.1 M, pH 7.6) alone and not mixed with 20% DMSO as solvent for these measurements. Indeed, this allowed to mimic the real operating conditions for these

fluorogenic compounds, to draw any relevant conclusions concerning their resistance to aggregation and their stability at physiological pH. As expected for conventional 3,6-diaryl-DPP dyes, and in line with the spectral parameters of several *N,N'*-dialkyl mono-(4'-pyridyl)-DPP dyes already determined in pure organic solvents (*e.g.*, DMF and MeCN) by Erbas and Alp [23], the three fluorophores **13**, **17** and **18** are characterized by a broad absorption within the blue-violet spectral range, centered at 467 nm, 471 nm and 439 nm respectively. The hypsochromic shift of the absorption wavelength of *N,N'*-dimethyl derivative **18** and the dramatic change in the shape of its absorption band (loss of symmetry and appearance of a shoulder) are attributed to the formation of non-emissive H-type aggregates. This hypothesis was supported by recording the excitation spectrum, which does not match the absorption spectrum (Fig. 2C). However, these aggregates are assumed to be disrupted for concentrations in the range 10^{-7} - 10^{-8} M (against 10^{-5} - 10^{-6} M for absorption measurements), typically used for recording emission/excitation spectra and determination of the relative fluorescence quantum yield. Thus, whatever *N*-lactam substituents (*i.e.*, carboxymethyl or methyl) of mono-(4'-pyridyl)-DPP scaffold, an intense fluorescence emission centered in the range 553-556 nm, was observed when the three pyridine-flanked DPP dyes (Ex. at 465 nm). Like *N,N'*-dialkyl mono-(4'-pyridyl)-DPP dyes being spectrally characterized in organic media [23], emission bands of **13**, **17** and **18** in PB are not structured and large Stokes' shift values are obtained. Very satisfactory values of fluorescence quantum yield in pure aq. medium have been determined. This is a valuable feature that enables to compensate the relatively low molar extinction coefficients of DPP fluorophores, in the perspective of practical applications in biological contexts. Obviously, this set of results also confirms that the best way to readily convert 3,6-diaryl-DPP pigments into fluorophores both soluble and strongly emissive in water, should be based on *N*-alkylation of their lactam groups with hydrophilic pendant arms. Indeed, this strategy leads to DPP molecules with a bolaamphiphilic character (*i.e.*, hydrophilic substituents located on both sides of the hydrophobic bis-lactam fused core) [24] not prone to micelle formation unlike amphiphilic dyes that are often non-emissive species. Unsurprisingly, the spectral behavior of *N,N'*-dihexyl derivative **21** in aq. buffer is dramatically different and unsatisfactory: weak fluorescence emission and persistence of aggregates even at low concentrations that prevents determination of relative fluorescence quantum yield in PB (Fig. S86). This latter result explains why the Hua group had been chosen a PBS-DMSO (8:2, v/v) mixture for the spectral measurements and *in vitro* validations of esterase- and γ -GT-sensitive probes **1** and **3** [7a, 7c]. The same medium was used for spectral characterization of **21** (Table

1, entry 10 and Fig. 87) but it is necessary to specify that addition of 20% DMSO in phosphate buffer changes greatly the pH value (8.5 vs. 7.6).

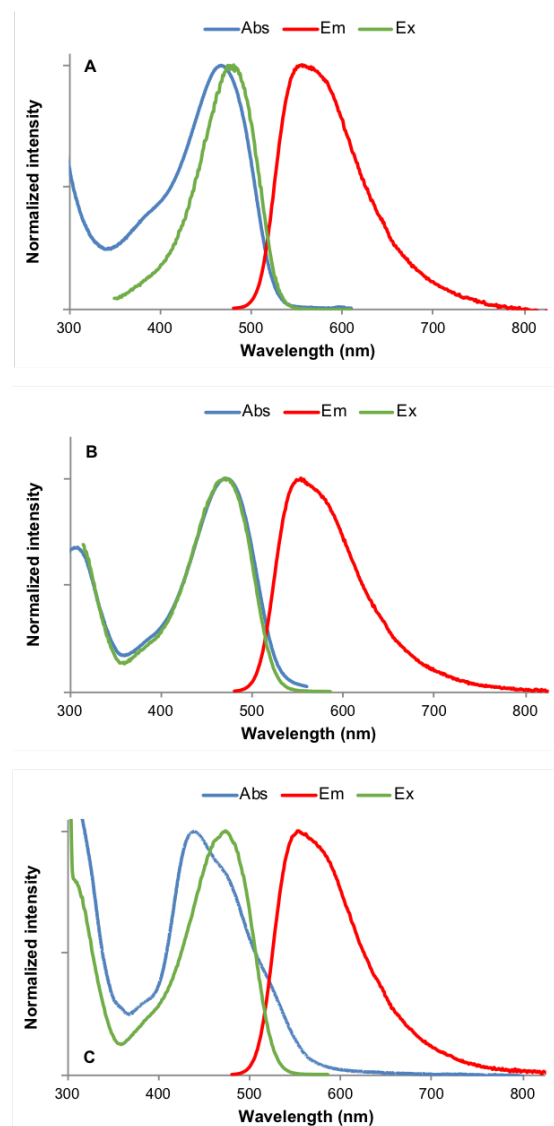


Fig. 2. Normalized absorption (blue), excitation (Em 625 nm for **13** or 600 nm for **17** and **18**, green) and emission (Ex. 465 nm, red) spectra of pyridine-flanked DPP fluorophores **13** (A), **17** (B) and **18** (C) in PB at 25 °C. *Please note: sample of **13** used for these photophysical characterizations contains less than 5% of non-fluorescent species **13-RO**.*

Table 1. Photophysical properties of pyridine-flanked DPP fluorophores and related enzyme-sensitive fluorogenic probes studied in this work, determined in PB (0.1 M, pH 7.6) at 25 °C.

Fluorophore or probe ^a	λ Abs (nm) ^b	λ Em. (nm)	ϵ (M ⁻¹ cm ⁻¹)	Stokes' shift (cm ⁻¹)	Φ_F ^c
7	516	669	14 050	4 432	- ^d
8	460	- ^e	20 500	- ^e	- ^e
9	529	675	16 250	4 089	- ^d
10	526	679	16 250	4 284	- ^d
11^f	531	613	9 300	2 519	- ^d

13^g	467	555	9 200	3 395	0.28
14	484	- ^e	13 100	- ^e	- ^e
17	471	553	13 650	3 148	0.50
18	439 (473) ^h	556	9 900 ^g	3 156	0.74
21^f	486	555	12 250	2 558	- ^d

^a stock solutions (1.0 mg/mL) of fluorophores and probes were prepared in spectroscopic grade DMSO.

^b only 0-0 band of the S₀→S₁ transition is reported.

^c for experimental conditions used for such determination, see supporting information.

^d non-linear relationship between area of Em. curve and Abs value at Ex. wavelength due to aq. instability or persistence of aggregates in diluted aq. solutions, has prevented determination of relative fluorescence quantum yield.

^e non-fluorescent.

^f spectral measurements were achieved in PB-DMSO (8:2, v/v, pH 8.5) due to poor solubility in pure phosphate buffer.

^g sample of **13** used for these photophysical characterizations contains less than 5% of non-fluorescent species **13-RO**.

^h formation of H-type aggregates that is disrupted for concentrations in the range 10⁻⁷-10⁻⁸ M used for the recording of Em./Ex. spectra. Ex. maximum is centered at 473 nm and Stokes' shift was calculated using this latter value.

When the same characterization methodology was applied to *N*-alkylpyridinium-based probes **7-11**, some common features have been noted and confirm that a strong ICT process operates within these DPP molecules: (1) broad structureless absorption and emission profiles with full-width at half maximum (FWHM) $\Delta\lambda_{1/2\max}$ in the range 100-115 nm and 125-130 nm respectively, (2) huge Stokes' shift values, and (3) NIR-I emission with a very low fluorescence quantum yield in aq. media (see Fig. 3B for the absorption/fluorescence spectra of **10** illustrating these spectral features). However, we did not manage to accurately determine this latter parameter due to the marked instability of **7** and **9-11** highlighted in PB and at low concentration (see section 3.5). The major consequence of the lack of a zero background signal for these fluorogenic probes, is that the detection of enzyme activity will be achieved through a ratiometric output signal and not an intensometric "OFF-ON" response [4b]. This will not be the case with the probe **8** that is functionalized with an azobenzene moiety knowing to act as an effective dark quencher through photochemical isomerization of its -N=N- bridge [16b, 25]. The lack of emission for **8** was borne out by fluorescence spectrum shown in Fig 3A.

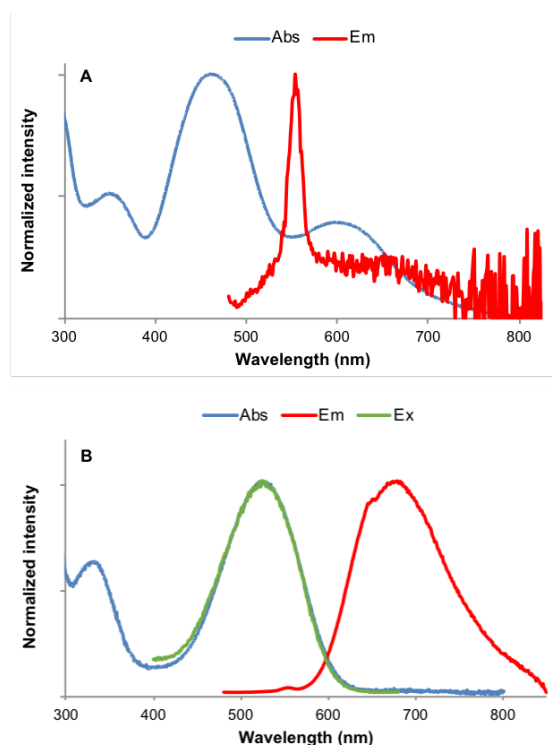


Fig. 3. Normalized absorption (blue), excitation (Em. 700 nm only for **10**, green) and emission (Ex. 465 nm, red) spectra of enzyme-sensitive fluorogenic probes **8** (A, target enzyme: AzoR) and **10** (B, targeted enzyme: PGA) in PB at 25 °C. Please note: probe **8** is not fluorescent and only the peak assigned to Raman scattering (553 nm) was observed.

3.5 Fluorogenic reactivity of enzyme-sensitive DPP-based probes. *In vitro* enzymatic assays

Due to commercial availability of NTR (recombinant, expressed in *E. coli*) and PGA (from *E. coli*), the fluorogenic reactivity of DPP-based probes **7** and **9-11** was readily studied through fluorescence-based *in vitro* assays involving time-course measurements and following reliable protocols previously used by us [26]. For azo-based fluorogenic probe **8**, a quite similar methodology was employed but using rat liver microsomes which are known to contain a wide range of redox enzymes including azoreductases [27]. Since these reductases are overexpressed and readily active only under hypoxic conditions, incubations with rat liver microsomes have been achieved with argon-saturated phosphate buffer. Control experiments (positive control) with fluorogenic azo-rosamine **MAR** [27a], whose bioreductive activation leads to the release of green-emitting rosamine **2Me RG**, have also been achieved to confirm the functionality of this *in vitro* biological model which will not involve the use of an isolated enzyme (see supporting information).

We first examined the three DPP-based probes rationally designed to be reactive towards hypoxia-related reductases (Fig. 4 and Figs. S88-S92). Somewhat surprisingly, incubation of *N*-(4-nitrobenzyl)pyridinium derivatives **7** and **9** with NTR/NADH at 37 °C did not produce a

significant and gradual increase of fluorescence emission centered at 555 nm (Ex. at 440 nm) indicating that the reduction of nitro group and the subsequent 1,6-benzyl elimination to release the mono-(4'-pyridyl)-DPP fluorophore **17** or **18**, is not triggered by this reductase (Fig. 4). We ruled out the hypothesis that NTR and/or its co-factor NADH are degraded by performing further kinetics highlighting rapid and effective bioreductive activation of 4-nitrobenzyl ether derived from a known NIR-I emitting phenol-based dihydroxanthene-hemicyanine dye (data not shown) [28]. The lack of reactivity of both probes towards NTR should be linked to their size and molecular geometry driven by the unique structure of DPP scaffold, that may prevent a favorable binding of **7** and **9** in the active site of this reductase. In our view, the presence of a positively-charged *N*-alkylpyridinium in close proximity to the enzyme-recognition moiety (*i.e.*, 4-nitrobenzyl) does not necessarily have an adverse effect on probe recognition by such reductase because several functioning NTR-responsive fluorescent probes bearing a bioreductive structural unit that is quite similar (*i.e.*, a 4-pyridyl substituent *N*-quaternized with (5-nitro-2-furyl)methyl group), have already reported in the literature [29].

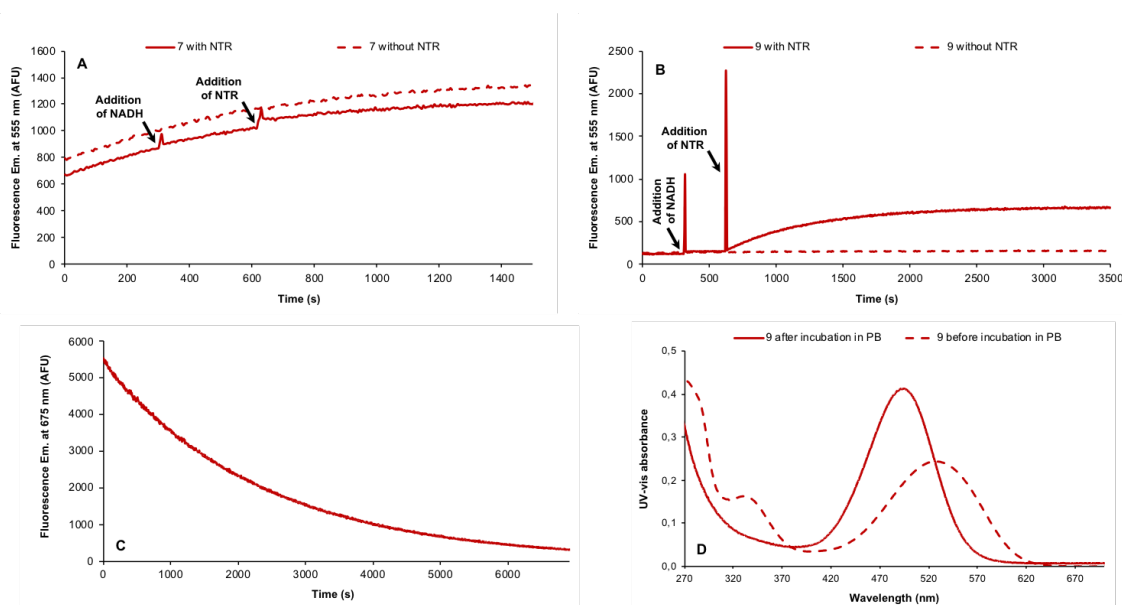


Fig. 4. Fluorescence emission time course (Ex./Em. 440/555 nm, slit 5 nm) of NTR-sensitive fluorogenic probes **7** (A) and **9** (B), concentration: 1.0 μ M, in the presence of NTR (0.1 U) and NADH (final concentration: 47 μ M) in PB at 37 $^{\circ}$ C. (C) Fluorescence emission time course (Ex./Em. 440/675 nm, slit 5 nm) of probe **9**, concentration: 1.0 μ M, in PB alone at 37 $^{\circ}$ C. (D) UV-vis absorption spectra of probe **9** before and after incubation in PB (12 h at 37 $^{\circ}$ C, concentration: 15 μ M).

A similar negative result was also obtained when AzoR-sensitive DPP probe **8** was incubated with rat liver microsomes and NADH under simulated hypoxic conditions. Indeed, no increase in green-yellow fluorescence intensity at 560 nm (Ex. at 465 nm) was observed, thus suggesting the inertness of azobenzene moiety towards these bioreductive conditions (Figs. S88 and S89). This was further supported by incubation of **8** with a large excess of sodium dithionite

(Na₂S₂O₄), a bio-compatible and effective reducing agent for diazo bridges highlighted by the Wagner group for applications in chemical biology [30], that did not produce the expected fluorescent "OFF-ON" response (Figs. S95 and S96). In addition to this lack of enzymatic activation, we noted a strange spectral behavior of these *N*-alkylpyridinium based probes when they are incubated in PB alone at 37 °C. A slow but gradual decrease of their NIR-I emission was observed, especially for **9**. As illustrated in Fig. 4C, fluorescence signal was significantly reduced by a factor of 17 within 115 min of incubation. Following this blank kinetics, the recording of absorption spectrum revealed the formation of a novel non-emissive species characterized by a blue-shifted maximum wavelength (-35 nm compared to starting probe **9**, Fig. 4D). Additional experiments have been done to gain insight into the mechanism of formation of this unknown product that may complicate the practical implementation of fluorogenic probes based on a pyridine-flanked DPP platform (*vide infra*). Curiously, this poor aq. stability observed in the absence of targeted enzyme, was not mentioned by the Hua group whereas their esterase- and γ -GT-activated ratiometric probes **1** and **3** share the same structural features than our probes [7a, 7c]. That point deserves further checking. All these disappointing results led us to unambiguously state that fluorogenic DPP dyes bearing a pyridyl moiety as optically tunable group are not really suitable candidates for designing bioreductive fluorescent imaging agents intended for hypoxia detection or bacterial monitoring.

Fortunately, the sensing performances of probe **10** toward hydrolase PGA have been much more encouraging. Indeed, when this phenylacetamide derivative was incubated with the commercial amidase, a moderately rapid and gradual increase of fluorescence emission at 555 nm (Ex. at 440 nm) was observed (Fig. 5A) and the plateau was reached within 2 h of incubation. Interestingly, a direct comparison of the fluorescence emission spectra of PGA-sensitive DPP probe **10** recorded before and after reaction with enzyme (Ex. at 440 nm, Fig. 5B), highlighted a spectral blue-shift of 120 nm allowing a proper ratiometric detection of PGA.

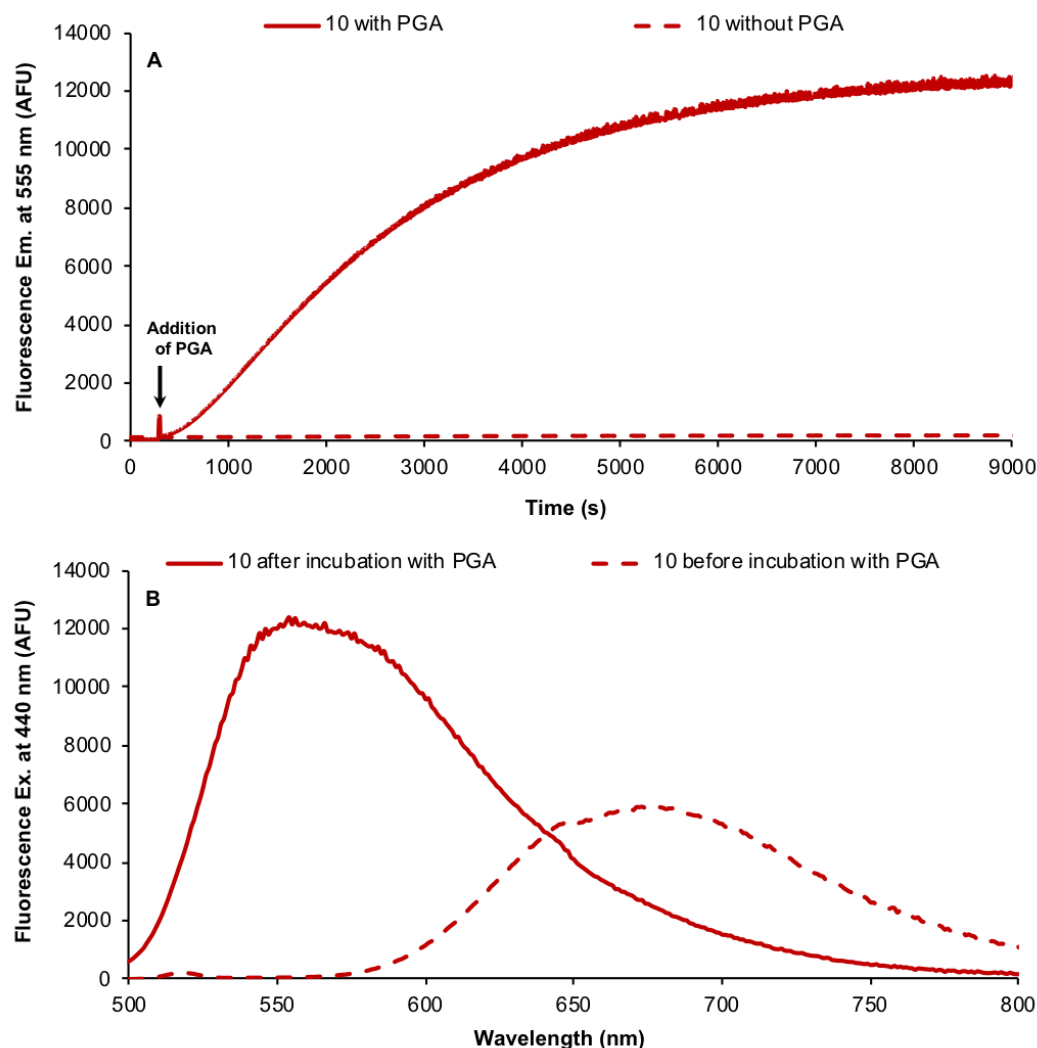


Fig. 5. (A) Fluorescence emission time course (Ex./Em. 440/555 nm, slit 5 nm) of PGA-sensitive fluorogenic probe **10**, concentration: 1.0 μM , in the presence of PGA (1 U) in PB at 37 $^{\circ}\text{C}$. (B) Fluorescence emission spectra (Ex. at 440 nm, slit 5 nm) of fluorogenic probe **10** before and after incubation with PGA (1 U, 150 min of incubation) in PB at 37 $^{\circ}\text{C}$.

In order to unambiguously confirm that the intense green-yellow fluorescence signal detected was due to the release of pyridine-flanked DPP dye **18**, this enzymatic reaction mixture and related blanks (*i.e.*, PB alone for HPLC column blank and **18** in PB alone) were subjected to RP-HPLC-fluorescence analyses (Fig. 6). As expected, a single peak ($t_{\text{R}} = 4.4$ min) was detected and assigned to the expected fluorophore (as proven by co-injection analysis with an authentic sample of **18**). Furthermore, this pyridine-flanked DPP was not detected in the blank reaction mixture (Figs. S109 and S110) thereby confirming that green-yellow fluorescence activation of the probe is solely triggered by PGA. It is important to point out that under our RP-HPLC conditions, *N*-alkylpyridinium probe **10** and parent DPP fluorophore **18** have the same retention time ($t_{\text{R}} = 4.4$ min). However, they can be readily differentiated according to the Ex./Em. channel used for fluorescence detection (*i.e.*, 520/675 nm for **10** and 475/550 nm for

18). Thus, we were able to highlight the conversion of the probe **10** into a non-fluorescent compound when it was subjected to a prolonged incubation in PB alone at 37 °C, because no peak was detected on both channels (Figs. S109 and S110). The corresponding kinetic curve obtained for this blank experiment, also emphasizes this non-enzymatic transformation, that appears to occur whatever the benzyl-like substituent carried by the 4'-pyridyl unit of DPP (*vide supra*, with NTR-sensitive probe **9**).

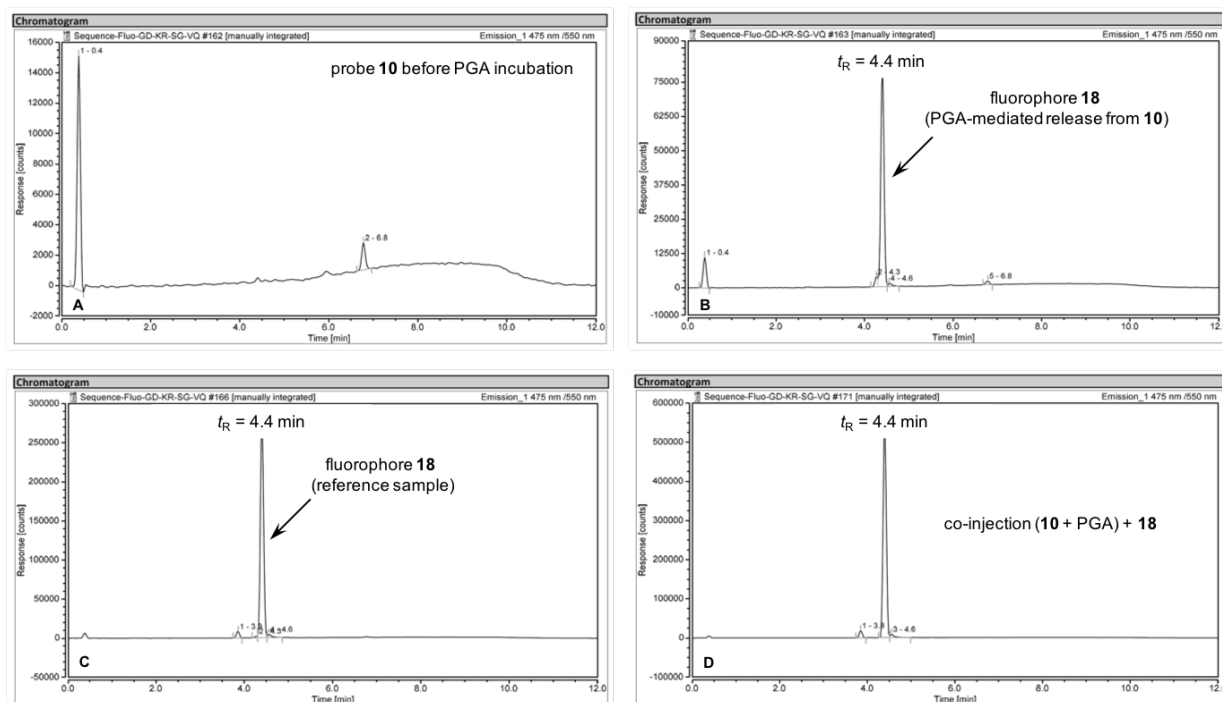


Fig. 6. RP-HPLC elution profiles (fluorescence detection Ex./Em. 475/550 nm) of PGA-sensitive fluorogenic probe **10** (A), enzymatic reaction mixture of probe **10** with PGA, 157 min of incubation at 37 °C (B), authentic sample of fluorophore **18** (C) and co-injection of enzymatic reaction mixture and **18** (D). Please note: minor peak at 6.8 min is present in the blank sample run.

These investigations were completed by RP-HPLC-MS analyses with the aim both of confirming the reaction between phenylacetamide-based probe **10** and PGA and of identifying the unknown product(s) arising from degradation of probes **9** and **10** in the lack of enzyme (Fig. 7 and Figs. S111-S116). First, the disappearance of the probe **10** and the formation of pyridine-flanked DPP **18** were clearly observed (Fig. 7), and the structure and integrity of this fluorophore were supported by UV-vis and MS-ESI+ data (both in "full scan" and single ion monitoring (SIM) modes; $t_R = 4.3$ min, MS(ESI+): m/z $[M + H]^+ = 396.1$ and 398.1 , calcd for $C_{19}H_{15}BrN_3O_2^+$ 396.0 and 398.0).

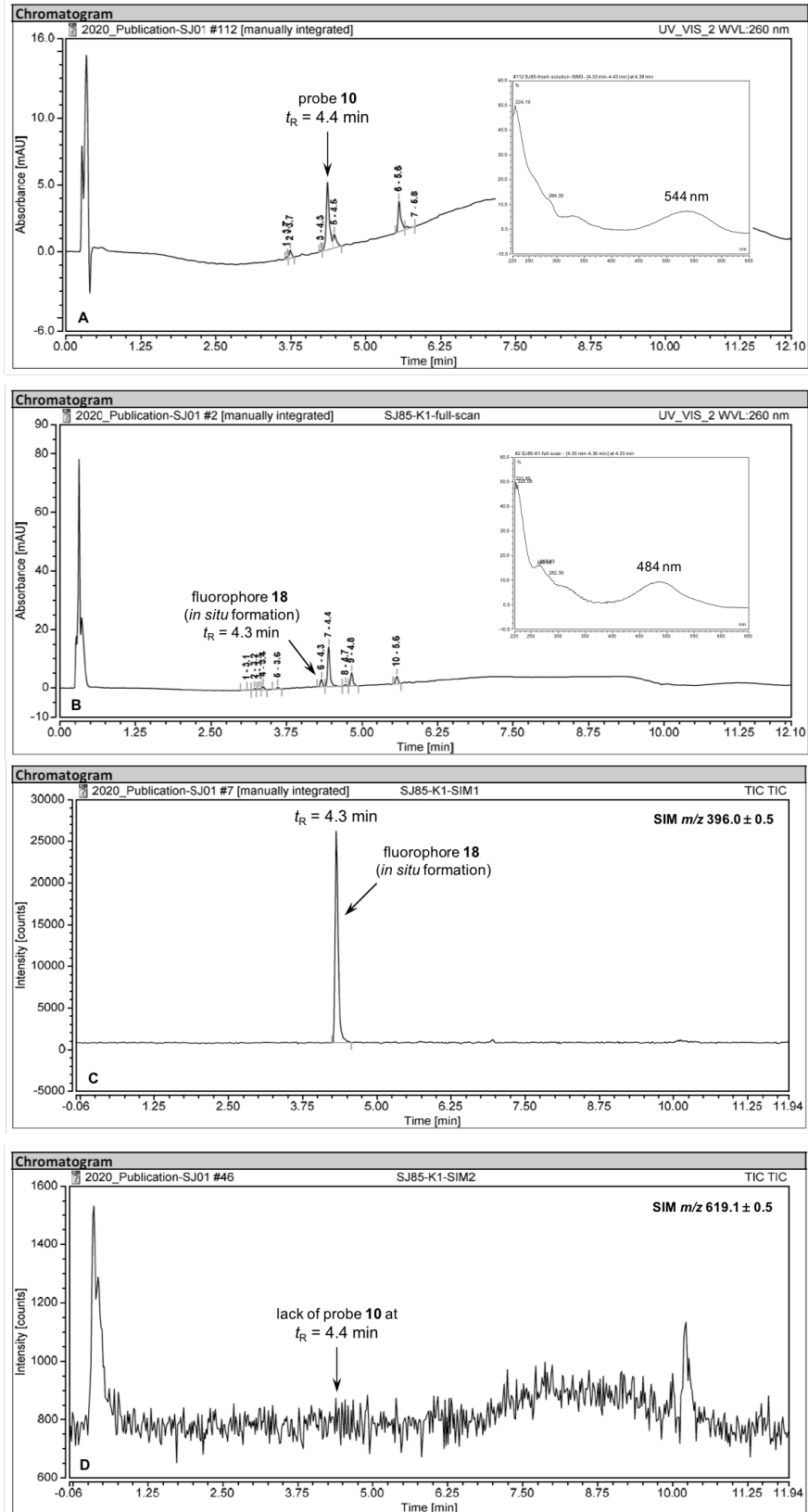


Fig. 7. RP-HPLC elution profiles of PGA-sensitive fluorogenic probe **10** before and after incubation with PGA. (A) UV detection at 260 nm of probe **10** in PB alone. (B) UV detection at 260 nm of probe **10** after enzymatic reaction. (C) ESI-MS detection, positive and SIM mode at $m/z = 396.0 \pm 0.5$ (detection of fluorophore **18**). (D) ESI-MS detection, positive and SIM mode at $m/z = 619.1 \pm 0.5$ (detection of probe **10**).

The RP-HPLC elution profile of blank mixture shows the lack of probe **10** ($t_R = 4.3\text{-}4.4$ min) and the appearance of a new major peak ($t_R = 3.2$ min) whose MS(ESI+) spectrum ("full scan") displays two pairs of ions at $m/z = 653.3/655.3$ and $671.3/673.0$ (Fig. 8).

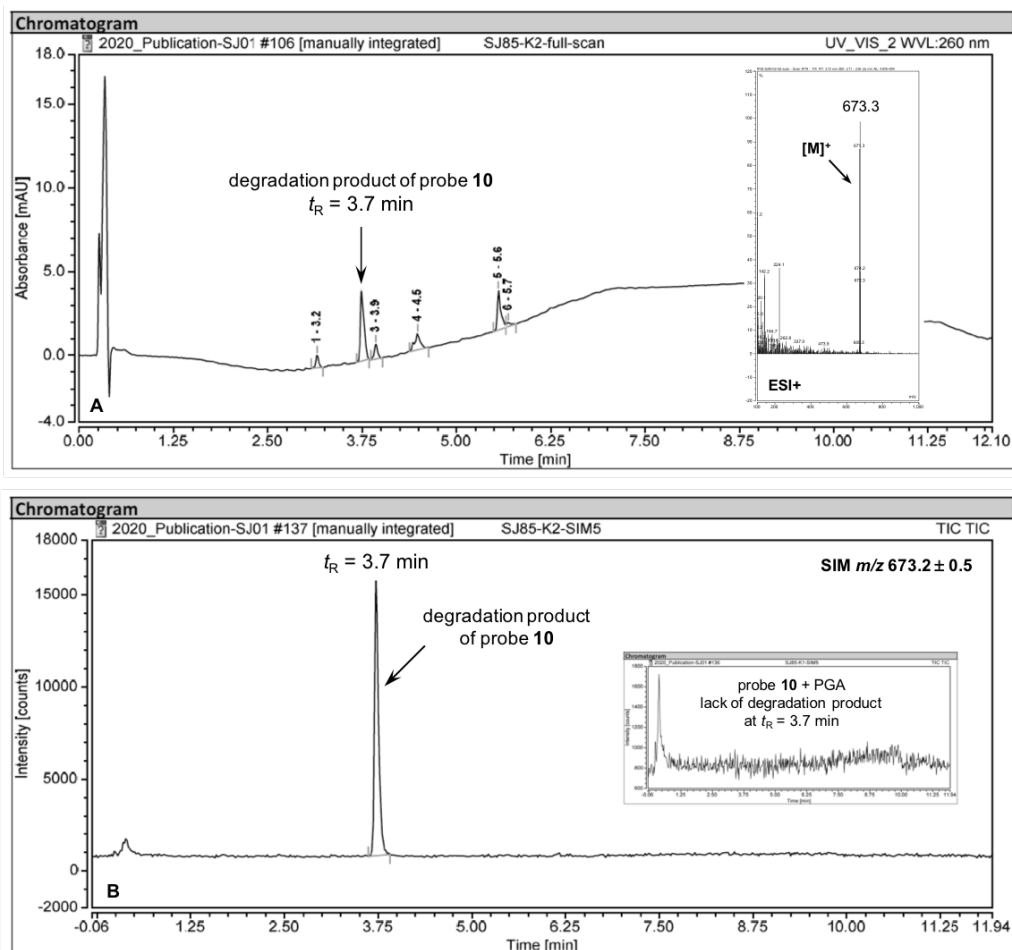


Fig. 8. RP-HPLC elution profiles of PGA-sensitive fluorogenic probe **10** after incubation in PB (0.1 M, pH 7.6) alone. (A) UV detection at 260 nm and ESI+ mass spectrum of peak at $t_R = 3.7$ min (inset). (B) ESI-MS detection, positive and SIM mode at $m/z = 673.2 \pm 0.5$; RP-HPLC elution profile of fluorogenic probe **10** after incubation with PGA, ESI-MS detection, positive and SIM mode at $m/z = 673.2 \pm 0.5$ (inset). Please note: complete description of isotopic pattern of $[M]^+$ of degradation product is omitted for clarity, $m/z = 671.3$ (90), 672.3 (30), 673.3 (100) and 674.2 (35).

Compared to pyridine-flanked DPP **18** (*vide supra*), this species was found to be much more easily detected in the positive mode, suggesting the integrity of *N*-alkylpyridinium moiety within its structure. If we assign peaks $653.2/655.3$ and $671.3/673.3$ to molecular ions the degradation product and its hydrated derivative respectively, the mass difference of $+34/+52$ amu with starting probe **10** suggests formal double/triple hydration and loss of two hydrogen atoms (to promote a ring aromatization?). The assumption that singlet oxygen, hypothetically formed by triplet energy transfer from *N*-alkylpyridinium-based DPP to molecular oxygen, could play a key role in this degradation pathway, was rapidly excluded because further blank experiments conducted under argon atmosphere or in the presence of sodium azide, a specific

quencher of singlet oxygen [31], also led to the formation of these degradation products (Figs. S115 and S116). Furthermore, the dramatic change in the absorption profile of probe **10**, already noted during *in vitro* bioassays of NTR-sensitive probe **9**, (*vide supra*), allowed us to conclude that the DPP chromophore is missing and probably degraded through hydrolytic ring-opening. In the light of these observations, we propose a hypothetical mechanism for the formation of furo[2,3-c]pyridinium derivatives **22** and **23** (Fig. 9), even if an additional, comprehensive study involving the independent synthesis and spectroscopic characterization of these unusual heterocyclic compounds, will be required. Once again, we are truly surprised that the Hua group did not discuss the hydrolysis problem of esterase- and γ -GT-sensitive probes **1** and **3** that is expected to occur in the same manner in PBS-DMSO (8:2, v/v) mixture whose pH is greater than 7.5 (*vide supra*) [7a, 7c].

A further control experiment aimed at proving the specificity of the enzymatic cleavage of PGA-sensitive probe **10**, was achieved. Incubation with an aminopeptidase (leucine aminopeptidase (LAP) from porcine kidney [32]) did not produce an increase of green-yellow fluorescence at 555 nm (Fig. S97), confirming that this latter protease is not able to cleave the phenylacetamide moiety. Furthermore, a direct comparison of the fluorescence emission spectra of **10** recorded before and after reaction with LAP (Ex. at 440 nm, Fig. S98) provided evidence once again of poor aq. stability of this *N*-alkylpyridinium-based probe.

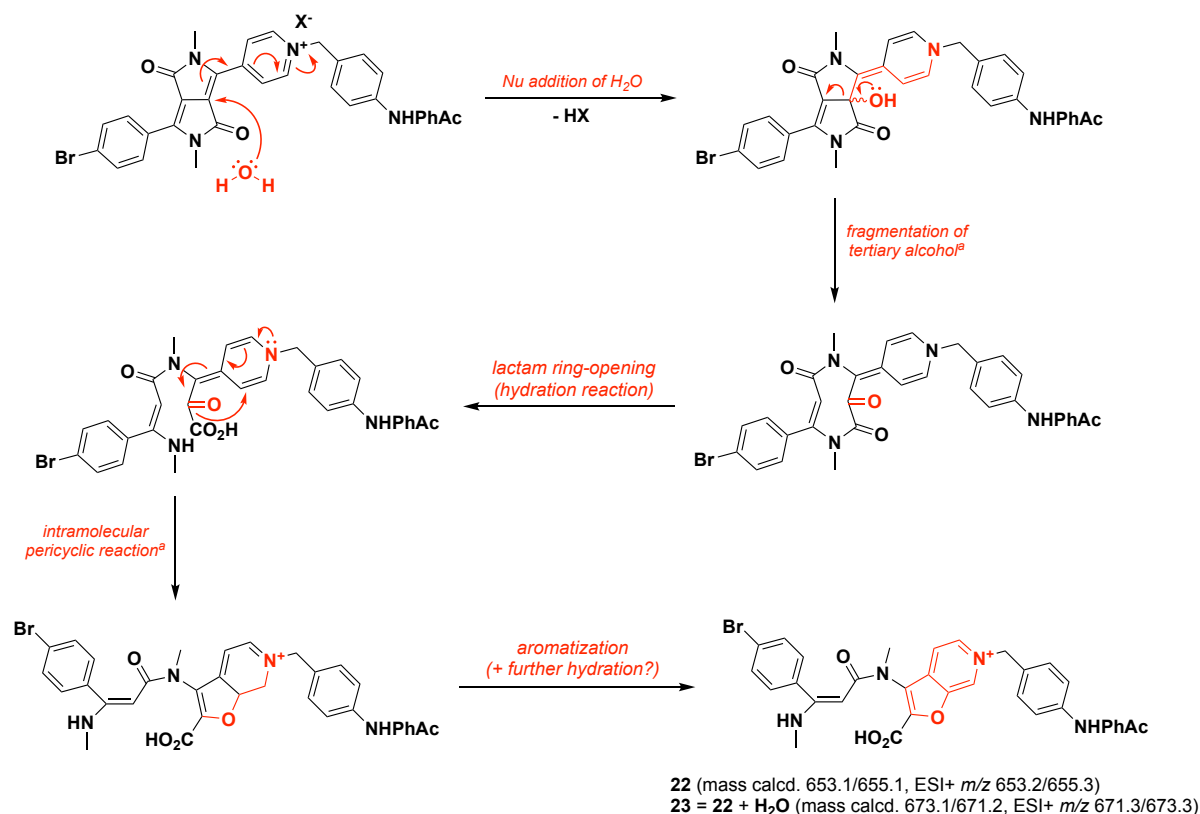


Fig. 9. Proposed degradation pathway of PGA-sensitive fluorogenic probe **10** observed in aq. buffers and in the lack of enzyme. "For clarity in the drawing of steps namely "fragmentation of tertiary alcohol" and "intramolecular pericyclic reaction", final protonation step of postulated carbanion intermediate is omitted. Please note: a similar degradation pathway may be proposed for NTR-sensitive fluorogenic probe **9**."

Finally, to assess the possible influence of *N*-lactam substituents on hydrolytic stability of probes based on *N*-alkylpyridinium-based DPP scaffold, more hydrophobic analog **21** bearing hexyl moieties was studied under the same conditions. As expected, intuitively, the spectral behavior and enzymatic reactivity of **11** were negatively impacted by the propensity of this compound to form aggregates in PB. The alternative use of PB-DMSO (8:2, v/v) as incubation buffer, did not produce better and valuable results in terms of ratiometric detection of PGA (Figs. S117 and S118). This confirmed the relevance of using polar or at least small size *N*-lactam substituents for fluorogenic DPP dyes used in the construction of reaction-based fluorescent probes working in biological media.

4. Conclusion

In an attempt to develop novel bioreductive fluorescent imaging agents with the aim of detecting tumor hypoxia, we assessed under-utilized photoactive platforms based on a DPP scaffold functionalized with one or two 4-pyridyl units acting as fluorogenic reactive center(s). We have synthesized four DPP-based fluorescent probes functionalized with either 4-nitrobenzyl or 4-[2-[4-(dimethylamino)phenyl]diazanyl]-benzyl moiety as NTR- or AzoR-responsive group respectively. *In vitro* study of all probes has highlighted on one hand the aq. instability of the dual-reactable NTR substrate **6** derived from a symmetrical 3,6-bis-(4'-pyridyl)-DPP dye and on the other hand the inability of both reductases (AzoR and NTR) to activate fluorogenic compounds based on a symmetrical mono-(4'-pyridyl)-DPP dye and designed by the protection-deprotection strategy (*i.e.*, masking-unmasking of pyridine nitrogen) [6]. Thus, we can conclude that pyridine-flanked DPP fluorophores are not well suited to construct "smart" activity-based probes for reductase-triggered hypoxia imaging. Conversely, and as already shown by the Hua group [7a, 7c], an effective fluorogenic ratiometric detection of hydrolases (*i.e.*, esterase and γ -GT previously studied by the Hua group and PGA in the present work) was readily achievable through an enzyme-triggered self-immolative *N*-dealkylation process of 4'-pyridinium moiety. In this context, we are convinced that structurally and easily functionalizable fluorogenic platforms such as mono-(4'-pyridyl)-DPP dyes may be a valuable alternative to more conventional aniline- or phenol-based fluorophores typically used

in the construction of fluorogenic probes for disease-relevant hydrolases. However, the issue of slow but effective degradation of *N*-alkylpyridinium-based DPP dyes in aq. media, unveiled by the present study, needs to be addressed before considering further applications in biological media. That is why we encourage (bio)chemists working in the field of enzyme-responsive fluorescent chemodosimeters to routinely implement an analytical methodology involving a series of RP-HPLC-fluorescence/MS analyses and along the lines of that used in this Article, especially for deciphering precisely their activation mechanism and possible degradation pathway(s), and thus improving their performances.

CRedit authorship contribution statement

Sébastien Jenni: Conceptualization, Investigation, Formal analysis, Writing - original draft.
Flavien Ponsot: Conceptualization, Investigation, Formal analysis, Writing - original draft.
Pierre Baroux: Investigation. **Lucile Collard:** Investigation. **Takayuki Ikeno:** Investigation.
Kenjiro Hanaoka: Formal analysis, Funding acquisition. **Valentin Quesneau:** Investigation.
Kévin Renault: Investigation. **Anthony Romieu:** Conceptualization, Investigation, Formal analysis, Writing - original draft, Writing - review & editing, Funding acquisition.

Declaration of competing interest

The authors declare that they have no known competing financial interests or personal relationships that could have appeared to influence the work reported in this paper.

Acknowledgements

This work is part of the project "Pharmacoinagerie et Agents Theranostiques", supported by the Université de Bourgogne and Conseil Régional de Bourgogne through the Plan d'Actions Régional pour l'Innovation (PARI) and the European Union through the PO FEDER-FSE Bourgogne 2014/2020 programs. Financial support from the French "Investissements d'Avenir" program, project ISITE BFC (contract ANR-15-IDEX-0003), especially for the post-doc fellowship of Dr. Sébastien Jenni, Agence Nationale de la Recherche (ANR, AAPG 2018, DetectOP_BChE, ANR-18-CE39-0014 and LuminoManufac-Oligo, ANR-18-CE07-0045), especially for the post-doc fellowships of Drs. Valentin Quesneau and Kévin Renault respectively is also greatly acknowledged. Flavien Ponsot gratefully acknowledges the French

Ministry of National Education, Higher Education and Research for his Ph. D. grant (2017-2020). This work was supported in part by JSPS KAKENHI Grant Numbers JP19H05414, JP20H04767, and JP16H05099 to Associate Prof. Kenjiro Hanaoka. GDR CNRS "Agents d'Imagerie Moléculaire" (AIM) 2037 is also thanked for its interest in this research topic. The authors thank the "Plateforme d'Analyse Chimique et de Synthèse Moléculaire de l'Université de Bourgogne" (PACSMUB, <http://www.wpcm.fr>) for access to analytical instrumentation, Dr. Myriam Laly (University of Burgundy, PACSMUB) for the determination of TFA content of samples purified by semi-preparative RP-HPLC, Prof. Daniel T. Gryko (Institute of Organic Chemistry, Polish Academy of Sciences, Warsaw, Poland) for his expert advice on the alkylation of pyridine-flanked DPP pigments, COBRA lab (UMR CNRS 6014), and Iris Biotech company for the generous gift of some chemical reagents used in this work. A special note of gratitude is also owed to all undergraduate or graduate students that occasionally participated to this research program: MM. Anthony Lenzi and Sullivan Guy (2018-2019), MM. Mathieu Bettinger and Tom Charenton (2019-2020) and Misses Emmanuelle Grimmonet and Lou Venne (2019-2020).

Supplementary data

Supplementary data to this article can be found online at <https://doi.org/10.1016/j.saa.2020.119179>.

References and note

A preprint was previously posted on ChemRxiv, see: <https://doi.org/10.26434/chemrxiv.13008524.v1>

- [1] a) D. G. Farnum, G. Mehta, G. G. I. Moore, F. P. Siegal, *Tetrahedron Lett.* 15 (1974) 2549-2552; b) M. Grzybowski, D. T. Gryko, *Adv. Optical Mater.* 3 (2015) 280-320.
- [2] For comprehensive reviews, see: a) A. Tang, C. Zhan, J. Yao, E. Zhou, *Adv. Mater.* 29 (2017) 1600013; b) W. Li, L. Wang, H. Tang, D. Cao, *Dyes Pigm.* 162 (2019) 934-950; c) Y. Patil, R. Misra, *J. Mater. Chem. C* 7 (2019) 13020-13031; d) X. Jiang, L. Wang, H. Tang, D. Cao, W. Chen, *Dyes Pigm.* 181 (2020) 108599.
- [3] a) J. B. Grimm, L. M. Heckman, L. D. Lavis, *Prog. Mol. Biol. Transl. Sci.* 113 (2013) 1-34; b) W. Sun, S. Guo, C. Hu, J. Fan, X. Peng, *Chem. Rev.* 116 (2016) 7768-7817; c) D. Cao, Z. Liu, P. Verwilst, S. Koo, P. Jangjili, J. S. Kim, W. Lin, *Chem. Rev.* 119 (2019) 10403-10519. Corrigendum: 119 (2019) 11550.
- [4] For selected reviews, see: a) J. Chan, S. C. Dodani, C. J. Chang, *Nat. Chem.* 4 (2012) 973-984; b) B. M. Luby, D. M. Charron, C. M. MacLaughlin, G. Zheng, *Adv. Drug Deliv. Rev.* 113 (2017) 97-121; c) S. Singha, Y. W. Jun, S. Sarkar, K. H. Ahn, *Acc.*

- Chem. Res. 52 (2019) 2571-2581; d) K. J. Bruemmer, S. W. M. Crossley, C. J. Chang, *Angew. Chem., Int. Ed.* 59 (2020) 13734-13762.
- [5] a) W. Qu, L. Yang, Y. Hang, X. Zhang, Y. Qu, J. Hua, *Sens. Actuators, B* 211 (2015) 275-282; b) S. Bi, G. Zhang, Y. Wu, S. Wu, L. Wang, *Dyes Pigm.* 134 (2016) 586-592; c) L. Wang, X. Chen, D. Cao, *Sens. Actuators, B* 244 (2017) 531-540; d) L. Wang, X. Chen, D. Cao, *New J. Chem.* 41 (2017) 3367-3373.
- [6] Y. Tang, D. Lee, J. Wang, G. Li, J. Yu, W. Lin, J. Yoon, *Chem. Soc. Rev.* 44 (2015) 5003-5015.
- [7] a) J. Wang, W. Xu, Z. Yang, Y. Yan, X. Xie, N. Qu, Y. Wang, C. Wang, J. Hua, *ACS Appl. Mater. Interfaces* 10 (2018) 31088-31095; b) J. Wang, L. Liu, W. Xu, Z. Yang, Y. Yan, X. Xie, Y. Wang, T. Yi, C. Wang, J. Hua, *Anal. Chem.* 91 (2019) 5786-5793; c) Z. Yang, W. Xu, J. Wang, L. Liu, Y. Chu, Y. Wang, Y. Hu, T. Yi, J. Hua, *J. Mater. Chem. C* 8 (2020) 8183-8190.
- [8] X. Li, X. Gao, W. Shi, H. Ma, *Chem. Rev.* 114 (2014) 590-659.
- [9] For selected examples, see: a) F. He, L. Liu, L. Li, *Adv. Funct. Mater.* 21 (2011) 3143-3149; b) H. Ftouni, F. Bolze, H. de Rocquigny, J.-F. Nicoud, *Bioconjugate Chem.* 24 (2013) 942-950; c) H. Ftouni, F. Bolze, J.-F. Nicoud, *Dyes Pigm.* 97 (2013) 77-83; d) S. Mula, D. Hablot, K. K. Jagtap, E. Heyer, R. Ziessel, *New J. Chem.* 37 (2013) 303-308; e) H. Shen, C. Kou, M. He, H. Yang, K. Liu, *J. Polym. Sci., Part A Polym. Chem.* 52 (2014) 739-751; f) E. Heyer, P. Lory, J. Leprince, M. Moreau, A. Romieu, M. Guardigli, A. Roda, R. Ziessel, *Angew. Chem. Int. Ed.* 54 (2015) 2995-2999.
- [10] X. Wu, W. Shi, X. Li, H. Ma, *Acc. Chem. Res.* 52 (2019) 1892-1904.
- [11] For comprehensive reviews, see: a) A. Alouane, R. Labruère, T. Le Saux, F. Schmidt, L. Jullien, *Angew. Chem., Int. Ed.* 54 (2015) 7492-7509; b) J. Yan, S. Lee, A. Zhang, J. Yoon, *Chem. Soc. Rev.* 47 (2018) 6900-6916.
- [12] For comprehensive reviews, see: a) W. Chyan, R. T. Raines, *ACS Chem. Biol.* 13 (2018) 1810-1823; b) H. Singh, K. Tiwari, R. Tiwari, S. K. Pramanik, A. Das, *Chem. Rev.* 119 (2019) 11718-11760; c) J. Zhang, X. Chai, X.-P. He, H.-J. Kim, J. Yoon, H. Tian, *Chem. Soc. Rev.* 48 (2019) 683-722.
- [13] G. R. Fulmer, A. J. M. Miller, N. H. Sherden, H. E. Gottlieb, A. Nudelman, B. M. Stoltz, J. E. Bercaw, K. I. Goldberg, *Organometallics* 29 (2010) 2176-2179.
- [14] C. Le Cocq, M.-A. Delsuc, J.-Y. Lallemand, *J. Chem. Soc., Chem. Commun.* (1981) 413-414.
- [15] T. Omura, R. Sato, *J. Biol. Chem.* 239 (1964) 2370-8.
- [16] For comprehensive reviews, see: a) R. B. P. Elmes, *Chem. Commun.* 52 (2016) 8935-8956; b) A. Chevalier, P.-Y. Renard, A. Romieu, *Chem. - Asian. J.* 12 (2017) 2008-2028; c) W. Qin, C. Xu, Y. Zhao, C. Yu, S. Shen, L. Li, W. Huang, *Chinese Chem. Lett.* 29 (2018) 1451-1455; d) R. Kumari, D. Sunil, R. S. Ningthoujam, N. V. A. Kumar, *Chem.-Biol. Interact.* 307 (2019) 91-104; e) Y.-L. Qi, L. Guo, L.-L. Chen, H. Li, Y.-S. Yang, A.-Q. Jiang, H.-L. Zhu, *Coord. Chem. Rev.* 421 (2020) 213460.
- [17] a) B. Mills, M. Bradley, K. Dhaliwal, *Clin. Transl. Imaging* 4 (2016) 163-174; b) M. M. Welling, A. W. Hensbergen, A. Bunschoten, A. H. Velders, H. Scheper, W. K. Smits, M. Roestenberg, F. W. B. van Leeuwen, *Clin. Transl. Imaging* 7 (2019) 125-138.
- [18] O. Vakuliuk, A. Purc, G. Clermont, M. Blanchard-Desce, D. T. Gryko, *ChemPhotoChem* 1 (2017) 243-252.
- [19] A. K. Chandel, L. V. Rao, M. L. Narasu, O. V. Singh, *Enzyme Microb. Technol.* 42 (2008) 199-207.
- [20] a) S. Gnaim, D. Shabat, *Acc. Chem. Res.* 47 (2014) 2970-2984; b) M. E. Roth, O. Green, S. Gnaim, D. Shabat, *Chem. Rev.* 116 (2016) 1309-1352.

- [21] a) J. Wang, Q. Chen, J. Wu, W. Zhu, Y. Wu, X. Fan, G. Zhang, Y. Li, G. Jiang, *New J. Chem.* 43 (2019) 6429-6434; b) L. Li, L. Feng, M. Zhang, X. He, S. Luan, C. Wang, T. D. James, H. Zhang, H. Huang, X. Ma, *Chem. Commun.* 56 (2020) 4640-4643; c) Z. Tian, L. Feng, L. Li, X. Tian, J. Cui, H. Zhang, C. Wang, H. Huang, B. Zhang, X. Ma, *Sens. Actuators, B* 310 (2020) 127872.
- [22] N. S. Sitnikov, Y. Li, D. Zhang, B. Yard, H.-G. Schmalz, *Angew. Chem., Int. Ed.* 54 (2015) 12314-12318.
- [23] S. C. Erbas, S. Alp, *J. Fluoresc.* 24 (2014) 329-335.
- [24] J.-H. Fuhrhop, T. Wang, *Chem. Rev.* 104 (2004) 2901-2938.
- [25] H. M. D. Bandara, S. C. Burdette, *Chem. Soc. Rev.* 41 (2012) 1809-1825.
- [26] a) S. Debieu, A. Romieu, *Org. Biomol. Chem.* 13 (2015) 10348-10361; b) G. Dejouy, K. Renault, Q. Bonnin, A. Chevalier, C. Michaudet, M. Picquet, I. E. Valverde, A. Romieu, *Org. Lett.* 22 (2020) 6494-6499.
- [27] a) W. Piao, S. Tsuda, Y. Tanaka, S. Maeda, F. Liu, S. Takahashi, Y. Kushida, T. Komatsu, T. Ueno, T. Terai, T. Nakazawa, M. Uchiyama, K. Morokuma, T. Nagano, K. Hanaoka, *Angew. Chem., Int. Ed.* 52 (2013) 13028-13032; b) A. Chevalier, W. Piao, K. Hanaoka, T. Nagano, P.-Y. Renard, A. Romieu, *Methods Appl. Fluoresc.* 3 (2015) 044004.
- [28] a) Y. Liu, L. Teng, L. Chen, H. Ma, H.-W. Liu, X.-B. Zhang, *Chem. Sci.* 9 (2018) 5347-5353; b) X. Tian, Z. Li, Y. Sun, P. Wang, H. Ma, *Anal. Chem.* 90 (2018) 13759-13766; c) F. Xu, H. Li, Q. Yao, H. Ge, J. Fan, W. Sun, J. Wang, X. Peng, *Chem. Sci.* 10 (2019) 10586-10594.
- [29] a) J. Xu, S. Sun, Q. Li, Y. Yue, Y. Li, S. Shao, *Analyst* 140 (2015) 574-581; b) X. You, L. Li, X. Li, H. Ma, G. Zhang, D. Zhang, *Chem. - Asian. J.* 11 (2016) 2918-2923; c) L. Yang, J.-Y. Niu, R. Sun, Y.-J. Xu, J.-F. Ge, *Sens. Actuators, B* 259 (2018) 299-306.
- [30] a) G. Leriche, G. Budin, L. Brino, A. Wagner, *Eur. J. Org. Chem.* (2010) 4360-4364; b) G. Leriche, G. Budin, Z. Darwich, D. Weltin, Y. Mely, A. S. Klymchenko, A. Wagner, *Chem. Commun.* 48 (2012) 3224-3226.
- [31] a) N. Miyoshi, G. Tomita, *Z. Naturforsch., B Anorg. Chem., Org. Chem.* 34B (1979) 339-43; b) N. Miyoshi, M. Ueda, K. Fuke, Y. Tanimoto, M. Itoh, G. Tomita, *Z. Naturforsch., B Anorg. Chem., Org. Chem.* 37B (1982) 649-52.
- [32] For a review on fluorescent probes for detection and bioimaging of LAP, see: Y. Chen, *Mater. Today Chem.* 15 (2020) 100216.